J. Am. Chem. Soc. 1991, 113, 3638–3649

Long-Lived Photoinitiated Charge Separation in Carotene–Diporphyrin Triad Molecules

Devens Gust,[*,†] Thomas A. Moore,[*,†] Ana L. Moore,[*,†] Feng Gao,[†] David Luttrull,[†] Janice M. DeGraziano,[†] Xiaochun C. Ma,[†] Lewis R. Makings,[†] Seung-Joo Lee,[†] Todd T. Trier,[†] Edith Bittersmann,[†] Gilbert R. Seely,[†] Susanne Woodward,[†] René V. Bensasson,[‡] Michel Rougée,[‡] Frans C. De Schryver,[§] and Mark Van der Auweraer[§]

Contribution from the Department of Chemistry and the Center for the Study of Early Events in Photosynthesis, Arizona State University, Tempe, Arizona 85287-1604, Laboratoire de Biophysique, ERA 951 du CNRS, Muséum National d'Histoire Naturelle, 75005 Paris, France, and Afdeling Organische Scheikunde, Katholieke Universiteit Leuven, Leuven, Belgium.

Received October 31, 1990

Abstract: A variety of molecular triads and dyads consisting of covalently linked carotenoid (C) and/or porphyrin (P) moieties have been prepared and studied with transient absorption and time-resolved fluorescence techniques. Diporphyrins of the type $\mathrm{P_A{-}P_B}$ and $\mathrm{C{-}P_A{-}P_B}$ triads demonstrate interporphyrin singlet–singlet energy transfer with rate constants ranging from 8.1×10^8 to 2.3×10^{10} s^{-1}. The energy-transfer rates are not in accord with those predicted by the Förster dipole–dipole theory, and it is suggested that energy transfer involves a contribution from an electron-exchange mechanism. Interporphyrin photoinitiated electron transfer is observed in molecules possessing sufficient thermodynamic driving force to produce $\mathrm{P_A{}^{\bullet+}{-}P_B{}^{\bullet-}}$ and $\mathrm{C{-}P_A{}^{\bullet+}{-}P_B{}^{\bullet-}}$ charge-separated states. The electron-transfer rate constant increases with increasing reaction free energy change for the molecules studied, and rate constants up to 3.5×10^9 s^{-1} and quantum yields up to 0.68 were measured. The carotenodiporphyrin triad systems undergo a subsequent electron-transfer step to give final $\mathrm{C^{\bullet+}{-}P_A{-}P_B{}^{\bullet-}}$ states. These states are rather long lived ($\tau \approx 250$ ns), and the overall quantum yields range up to 0.32.

Photoinitiated transmembrane electron transfer to yield long-lived charge-separated states is the basic energy conversion process of photosynthesis. In the protein environment of photosynthetic reaction centers, it is carried out by a series of short-range, fast and efficient electron-transfer steps, which move the electron and the hole to opposite sides of the membrane. The actual photochemistry involves chlorophyll derivatives, quinones, and other small organic molecules. In photosynthetic bacteria, the primary steps consist of photoinitiated electron transfer between cyclic tetrapyrrole molecules: the special pair of bacteriochlorophylls, a bacteriopheophytin, and possibly an accessory bacteriochlorophyll.[1] Singlet energy transfer between tetrapyrroles is also important in photosynthesis. Antenna systems consisting of arrays of chlorophyll, carotenoid, or other chromophores funnel singlet excitation energy to the reaction center.

Synthetic multicomponent molecules that mimic both of these processes have been reported. For example, covalently linked porphyrin–quinone dyads have been extensively studied from the point of view of photoinitiated electron transfer.[2] We have previously reported a variety of three- and four-part molecular devices consisting of porphyrins (P) linked to quinone electron acceptors (Q) and carotenoid polyenes (C), which successfully mimic the multistep electron-transfer strategy of the reaction center to generate long-lived charge-separated states.[3] However, in all of these systems, the photoinitiated transfer occurred between an excited porphyrin molecule and a quinone, rather than between tetrapyrroles. Other researchers have prepared a variety of molecules containing two or more tetrapyrrole moieties. These demonstrate singlet energy and occasionally photoinitiated electron-transfer behavior[4–16] but fail to yield long-lived charge separation.

We recently described a carotene–diporphyrin–diquinone ($\mathrm{C{-}P{-}P{-}Q_A{-}Q_B}$) molecular device that undergoes electron transfer from the porphyrin first excited singlet state to yield $\mathrm{C{-}P{-}P^{\bullet+}{-}Q_A{}^{\bullet-}{-}Q_B}$.[17] This state then decays to a very long lived (340 μs) charge-separated state of the form $\mathrm{C^{\bullet+}{-}P{-}P{-}Q_A{-}Q_B{}^{\bullet-}}$. The formation of an interporphyrin electron-transfer state ($\mathrm{C{-}P^{\bullet+}{-}P^{\bullet-}{-}Q_A{-}Q_B}$) was not observed because this state is several hundred millielectronvolts higher in energy than the porphyrin first excited singlet states at 1.90 eV. Similar results were obtained for several other pentad[17] and tetrad[18–20] molecules. Thus, the energy of the interporphyrin electron-transfer state must be lowered if it is to be populated from the porphyrin singlet state.

[†] Arizona State University.
[‡] Muséum National d'Histoire Naturelle.
[§] Katholieke Universiteit Leuven.

(1) For general reviews, see: Kirmaier, C.; Holten, D. *Photosynth. Res.* **1987**, *13*, 225. Feher, G.; Allen, J. P.; Okamura, M. Y.; Reese, D. C. *Nature (London)* **1989**, *339*, 111.

(2) For reviews, see: Connolly, J. S.; Bolton, J. R. In *Photoinduced Electron Transfer, Part A.*; Fox, M. A., Channon, M., Eds.; Elsevier: Amsterdam, 1988; Chapter 6.2. Wasielewski, M. R. *Ibid.* Chapter 1.4. Wasielewski, M. R. *Photochem. Photobiol.* **1988**, *47*, 923.

(3) For reviews, see: Gust, D.; Moore, T. A. *Science (Washington, D.C.)* **1989**, *244*, 35; Gust, D.; Moore, T. A. *Top. Curr. Chem.* in press; Gust, D.; Moore, T. A. *Adv. Photochem.*, in press.

(4) For reviews, see refs 5–9. For examples, see refs 10–16.

(5) Harriman, A. In *Supramolecular Photochemistry*; Balzani, V., Ed.; D. Reidel: Boston, 1987; p 207.

(6) Boxer, S. G. *Biochim. Biophys. Acta* **1983**, *726*, 265.

(7) Harriman, A. In *Energy Resources Through Photochemistry and Catalysis*; Gratzel, M., Ed.; Academic Press: New York, 1983; Chapter 6.

(8) Dolphin, D.; Hiom, J.; Paine, J. B., III *Heterocycles* **1981**, *16*, 417.

(9) Sakata, Y. *Yuki Gosei Kagaku Kyokai Shi* **1981**, *39*, 909.

(10) Sakata, Y.; Nishitani, A.; Nishimizu, N.; Misumi, S.; McIntosh, A. R.; Bolton, J. R.; Kanda, Y.; Karen, A.; Okada, T.; Mataga, N. *Tetrahedron Lett.* **1985**, *26*, 5207.

(11) Dubowchik, G. M.; Hamilton, A. D. *J. Chem. Soc., Chem. Commun.* **1986**, 1391 and references cited therein.

(12) Cowan, J. A.; Sanders, J. K. M.; Beddard, G. S.; Harrison, R. J. *J. Chem. Soc., Chem. Commun.* **1987**, 55.

(13) Cowan, J. A.; Sanders, J. K. M. *J. Chem. Soc., Chem. Commun.* **1985**, 1214.

(14) (a) Sessler, J. L.; Hugdahl, J.; Johnson, M. R. *J. Org. Chem.* **1986**, *51*, 2828. (b) Sessler, J.; Johnson, M. R. *Recl. Trav. Chim. Pays-Bas* **1987**, *106*, 222.

(15) Mataga, N.; Yao, H.; Okada, T.; Kanda, Y.; Harriman, A. *Chem. Phys.* **1989**, *131*, 473.

(16) Nagata, T.; Osuka, A.; Maruyama, K. *J. Am. Chem. Soc.* **1990**, *112*, 3054.

(17) Gust, D.; Moore, T. A.; Moore, A. L.; Lee, S.-J.; Bittersmann, E.; Luttrull, D. K.; Rehms, A. A.; DeGraziano, J. M.; Ma, X. C.; Gao, F.; Belford, R. E.; Trier, T. T. *Science (Washington, D.C.)* **1990**, *248*, 199.

(18) Gust, D.; Moore, T. A.; Moore, A. L.; Barrett, D.; Harding, L. O.; Makings, L. R.; Liddell, P. A.; De Schryver, F. C.; Van der Auweraer, M.; Bensasson, R. V.; Rougée, M. *J. Am. Chem. Soc.* **1988**, *110*, 321.

(19) Gust, D.; Moore, T. A.; Moore, A. L.; Seely, G.; Liddell, P. A.; Barrett, D.; Harding, L. O.; Ma, X. C.; Lee, S.-J.; Gao, F. *Tetrahedron* **1989**, *45*, 4867.

(20) Gust, D.; Moore, T. A.; Moore, A. L.; Makings, L. R.; Seely, G. R.; Ma, X. C.; Trier, T. T.; Gao, F. *J. Am. Chem. Soc.* **1988**, *110*, 7567.

0002-7863/91/1513-3638$02.50/0

This in turn requires changes in the redox properties of the individual porphyrin moieties. One strategy for doing this is to retain the basic *meso*-tetraarylporphyrin structure but to incorporate electron-withdrawing or electron-donating groups on the aryl rings and/or the porphyrin macrocycle in order to stabilize the porphyrin radical anions or cations, respectively.[21-23]

Carotenodiporphyrin triads **1** and **2** and diporphyrins **3**–**7** have now been prepared in order to investigate this strategy. Each of the C–P–P molecules features two *p*-tolyl groups on the porphyrin bearing the carotenoid (to stabilize a positive charge on the porphyrin) and three electron-withdrawing pentafluorophenyl groups on the second porphyrin (to stabilize a negative charge). Thus, the systems are electrochemically biased for unidirectional photoinitiated electron transfer. As discussed below, excitation of these molecules yields porphyrin first excited singlet states, which may transfer singlet excitation to the attached porphyrin and/or donate or accept an electron to form an initial charge-separated state (C–$P^{•+}$–$P^{•-}$). A subsequent electron-transfer step yields a final $C^{•+}$–P–$P^{•-}$ state. The final state has a lifetime of up to 250 ns and is formed with a quantum yield of up to 0.32, depending upon the structure of the molecule.

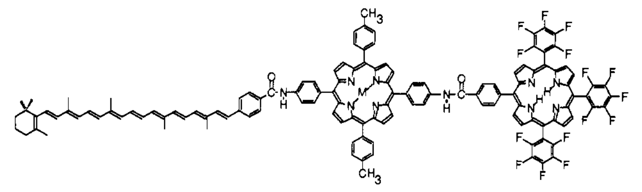

1: M = Zn

2: M = H_2

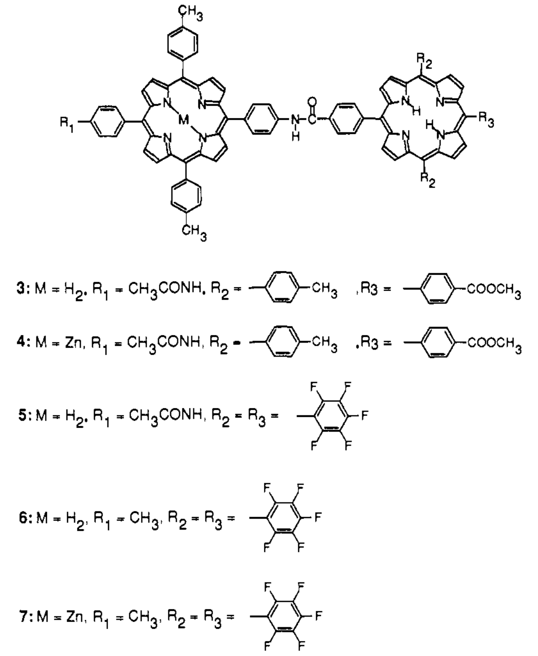

Results and Discussion

The syntheses of **1**–**7** and related model systems and their characterization with UV-vis, NMR, and mass spectrometric techniques are reported in the Experimental Section. Investigation of the photochemistry of the triads and dyads began with an examination of the steady-state absorption and emission spectra. Time-resolved fluorescence studies allowed determination of the rate constants for energy and photoinitiated electron transfer. Transient absorption studies on the nanosecond time scale gave the yields and lifetimes of the $C^{•+}$–P_A–$P_B^{•-}$ states. Finally, cyclic voltammetric studies allowed estimation of the energies of the various charge-separated states. The results of these studies for each molecule in the series are reported below.

Diporphyrin 3. The two porphyrin moieties of **3** are closely related, and in dichloromethane solution the absorption spectra of model porphyrin monomers **8** and **9** are very similar. The spectrum of **3** in dichloromethane is identical with a linear combination of those of **8** and **9**, within experimental error, and features four Q-bands at 518, 554, 594, and 650 nm and a Soret absorption at 422 nm. Thus, linkage of the chromophores does not lead to significant changes in absorption band wavelengths, widths, or relative extinction coefficients.

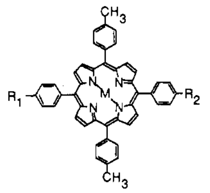

8: $R_1 = R_2 = CH_3CONH$-, M = H_2

9: $R_1 = R_2 =$ -$COOCH_3$, M = H_2

10: $R_1 =$ -CH_3, $R_2 = CH_3CONH$-, M = Zn

Interpretation of the photochemistry and photophysics of the dyads and triads is facilitated by a knowledge of their solution conformations. The partial double bond character of the amide linkage in **3** would be expected to restrict the molecule to extended conformations in which the two porphyrin moieties are directed out, away from one another, rather than folded arrangements with the porphyrin π-electron systems stacked in close contact. This conclusion is supported by 400-MHz ^1H NMR investigations. The aromatic ring current effects in porphyrins are very large, and the chemical shifts of hydrogen nuclei are therefore sensitive functions of their location with respect to a porphyrin macrocycle.[24,25] In the case of **3**, the hydrogen nuclei do not exhibit the shielding, relative to model compounds, that would be expected if a folded conformation were present (see Experimental Section). In addition, 2D NOE studies of a closely related molecule show no interporphyrin NOE effects. Of course, rotation about the single bonds in the linkage should be relatively facile, and as a result, although the interporphyrin separation is well-defined (center to center distance ca. 19 Å), the interporphyrin dihedral angles are currently unknown.

The corrected fluorescence emission spectrum of **3** in dichloromethane with excitation at 420 nm is also similar to those of **8**, **9**, and tetraphenylporphyrin itself[26] and features two maxima at 655 and 720 nm in a ratio of intensities of 2.2 to 1.

Time-resolved fluorescence studies of **3** in dichloromethane were performed with use of the single-photon timing technique. Details are presented in the Experimental Section. Excitation of **3** at 590 nm yielded a decay that could be satisfactorily analyzed as a single exponential with a lifetime of 7.8 ns ($\chi^2 = 1.12$). This lifetime is nearly the same as those observed for model porphyrins **8** (7.9 ns) and **9** (8.3 ns). Thus, photoinitiated electron-transfer quenching of the porphyrin singlet states is insignificant.

The reason for the lack of photoinitiated electron transfer in **3** becomes apparent upon examination of the energies of the relevant excited and charge-separated states as shown in Scheme I. The energies of the porphyrin first excited singlet states have been calculated from the average of the frequencies of the longest wavelength absorption maxima and the shortest wavelength emission maxima (Table I). The energy of the $P_A^{•+}$–$P_B^{•-}$ charge-separated state has been estimated from the first oxidation

---

[21] Worthington, P.; Hambright, P.; Williams, R. F. X.; Reid, J.; Burnham, C.; Shamim, A.; Turay, J.; Bell, D. M.; Kirkland, R.; Little, R. G.; Datta-Gupta, N.; Eisner, U. *J. Inorg. Biochem.* **1980**, *12*, 281.

[22] Giraudeau, A.; Callot, H. J.; Gross, M. *Inorg. Chem.* **1979**, *18*, 201.

[23] Kadish, K. M.; Morrison, M. M. *J. Am. Chem. Soc.* **1976**, *98*, 3326.

[24] Chachaty, C.; Gust, D.; Moore, T. A.; Nemeth, G. A.; Liddell, P. A.; Moore, A. L. *Org. Magn. Reson.* **1984**, *22*, 39.

[25] Abraham, R. J.; Bedford, G. R.; McNeillie, D.; Wright, B. *Org. Magn. Reson.* **1980**, *14*, 418.

[26] Gouterman, M. In *The Porphyrins*; Dolphin, D., Ed.; Academic Press: New York, 1978; Vol. III, Chapter 1.

Scheme I

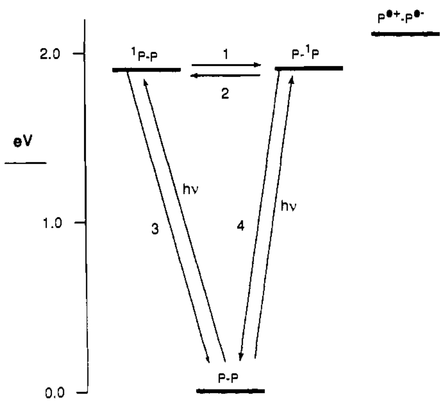

Table I. First Excited Singlet State Energies and Redox Potentials (vs SCE)[a] for Triads, Dyads, and Model Compounds

compd	^1P (eV)	E_r^2 (V)	E_r^1 (V)	E_o^1 (V)	E_o^2 (V)
13[b]	1.90	−1.53[c]	−1.20	0.66[c]	
8[b]	1.90	−1.52	−1.18	0.95	1.14
15	2.09		−1.36	0.74	1.17
9	1.90	−1.47	−1.16	1.06	1.36
14	1.90		−1.20	0.96	1.28
10	2.09			0.77	1.18
11	1.93	−1.24	−0.85	1.48	1.72
3	1.90, 1.90	−1.51[c]	−1.16	1.03	1.21
4	2.09, 1.90				
5	1.90, 1.93	−1.21	−0.86	0.91	1.39
6	1.90, 1.93				
7	2.09, 1.93		−0.80	0.81	1.15

[a] Cyclic voltammetry potentials were measured against an internal ferrocene reference and extrapolated to zero scanning rate. The values obtained were converted to potentials vs SCE by adding 0.48 to the ferrocene values. [b] From ref 30. [c] Irreversible.

potential of **8** and the first reduction potential of **9**, as determined from cyclic voltammetric measurements (see Experimental Section). These potentials also appear in Table I. No correction for any possible stabilization due to coulombic effects has been attempted. It is clear from the scheme and Table I that whereas the $P_A^{\bullet+}$–$P_B^{\bullet-}$ state lies at about 2.11 eV above the ground state, the porphyrin first excited singlet states are at only 1.90 eV. Thus, photoinitiated electron transfer is endergonic by about 0.2 eV and would be expected to be slow. The porphyrin first excited singlet states relax by the usual intersystem crossing, internal conversion, and fluorescence mechanisms (represented by steps 3 and 4 in Scheme I).

Diporphyrin 4. Dyad **4** is structurally identical with **3**, except that the central hydrogen atoms in the porphyrin bearing the acetamido group have been replaced by zinc. The absorption spectrum of this molecule features Q-band maxima at 516, 552, 590, and 650 nm, whereas the Soret appears as a single maximum at 422 nm. The absorption spectrum is again a linear combination of the spectra of the component chromophores.

In emission, however, the situation is quite different. Figure 1 shows the corrected fluorescence spectra of **4** and model porphyrins **9** and **10** in dichloromethane solution. The zinc porphyrin **10** has maxima at 600 and 648 nm, whereas the free base **9** has two maxima at 654 and 718 nm. The emission spectrum of dyad **4** resembles that of the free base porphyrin, with no significant emission from the zinc porphyrin moiety, even though both porphyrin species absorb at the excitation wavelength (550 nm). This result suggests efficient and therefore rapid singlet–singlet energy transfer from the zinc porphyrin to the free base. This process is shown as step 1 in Scheme II, which illustrates the relevant excited and charge-separated states for **4**.

Confirmation of singlet energy transfer was obtained from time-resolved fluorescence studies. Excitation of a dichloromethane solution of **4** was performed at 590 nm, and decays were measured at 10 wavelengths in the 630–730-nm region. The results from all 10 decays were analyzed together with use of a global technique[27] in order to obtain the best fit to three exponential decay times. Fits to two exponentials were not satisfactory. The three lifetimes obtained were 0.042, 1.5, and 7.9 ns (global $\chi^2 = 1.08$). The relative amplitudes of the three components at each wavelength were scaled to the corrected steady-state emission spectrum to yield the decay-associated spectrum shown in Figure

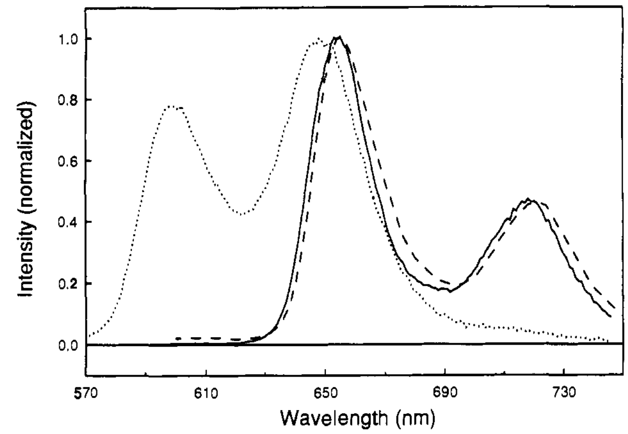

Figure 1. Key: dashed line, corrected fluorescence emission spectrum of diporphyrin **4** in dichloromethane solution with excitation at 550 nm; solid line, corresponding emission spectrum of free base porphyrin monomer **9**; dotted line, emission spectrum of monomeric zinc porphyrin **10** in the same solvent. The spectra have been normalized at the maxima. Note that the spectrum of the diporphyrin is nearly identical with that of the free base model system, with little contribution from the zinc porphyrin moiety.

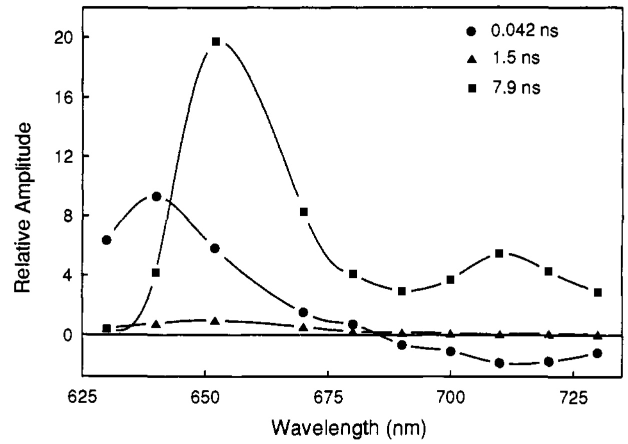

Figure 2. Decay-associated spectra for diporphyrin **4** in dichloromethane solution with excitation at 590 nm. The three components of the decay were determined by a global analysis of decays taken at the 10 indicated wavelengths (global $\chi^2 = 1.08$).

Scheme II

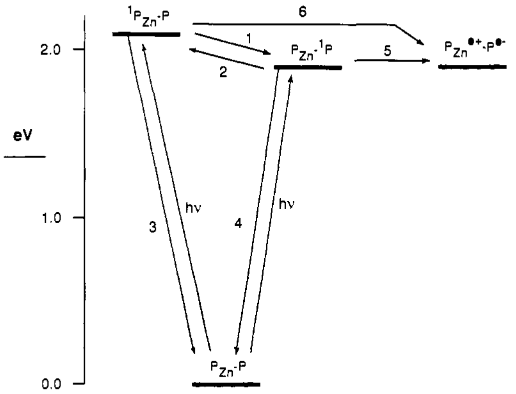

---

(27) Wendler, J.; Holzwarth, A. R. *Biophys. J.* **1987**, *52*, 717.

2. It can be seen from the figure that the 1.5-ns component of the decay is quite small in amplitude. It likely represents a minor impurity and will be ignored.[28] The short component of 42 ps makes a large positive contribution to the decay in the 630–660-nm region, where zinc porphyrin emits strongly, and a significant negative contribution (growth of fluorescence) in the 710-nm region, where the emission is due mainly to the free base porphyrin. Thus, this component denotes the proposed singlet–singlet energy transfer from the zinc porphyrin to the free base moiety. The lifetime of the zinc porphyrin first excited singlet state is therefore 0.042 ns. The 7.9-ns component of the decay has a spectrum similar to that of a free base porphyrin and thus represents the decay of the first excited singlet state of the porphyrin bearing the methyl ester group.

Turning to Scheme II, we see that the significant energy gap between the zinc porphyrin first excited singlet state at 2.08 eV and that of the free base at 1.90 eV means that singlet energy transfer from the free base to the zinc porphyrin via step 2 should be very slow, relative to step 1. Thus, assuming that the shortening of the lifetime of the zinc porphyrin first excited singlet state in **4** is due solely to energy transfer, the singlet–singlet energy-transfer rate constant for step 1 (k_1) may be estimated from

$$k_1 = \frac{1}{\tau} - \frac{1}{\tau_0} \qquad (1)$$

where τ is the lifetime of the zinc porphyrin first excited singlet state in the dyad (0.042 ns) and τ_0 is the lifetime of the zinc porphyrin singlet state of a model compound that lacks the singlet energy transfer possibility but otherwise has similar photochemical parameters. In dichloromethane solution, zinc porphyrin **10** has an excited singlet lifetime of 1.6 ns. Using this value, we calculate a singlet–singlet energy transfer-rate constant k_1 of 2.3×10^{10} s^{-1} for **4**. The quantum yield of energy transfer Φ_1 is given by

$$\Phi_1 = \tau k_1 \qquad (2)$$

and equals 0.97. An identical singlet–singlet energy-transfer rate constant was recently determined for a molecular pentad of the form C–P$_{Zn}$–P–Q–Q, where the diporphyrin portion of the molecule was similar to **4** in structure.[17]

The 7.9-ns component of the decay-associated spectrum in Figure 2 represents the decay of the free base porphyrin first excited singlet state. The lifetime of this state is similar to that of **9** (8.3 ns). Thus, no additional decay pathways of significance have resulted from the linkage of the two porphyrin moieties, and the free base moiety of **4** decays in the same ways as the model unlinked porphyrin. This result verifies our assumption of slow singlet–singlet energy transfer from the free base to the zinc porphyrin via step 2 in Scheme II. In fact, treating the interconversion of the two excited singlet states as an equilibrium process

$$\Delta G^\circ = -RT \ln K = -0.18 \text{ eV} \qquad (3)$$

where K is the equilibrium constant for energy transfer and equals 1100 at 298 K. Thus, k_2 is 2.1×10^7 s^{-1}.

The fact that **9** and the free base moiety of **4** have similar first excited singlet state lifetimes also shows that the free base first excited singlet state of **4** does not undergo significant photoinitiated electron transfer to yield $P_{Zn}^{\bullet+}$–$P^{\bullet-}$, as per step 5 in Scheme II. Examination of the scheme shows that the two states are virtually isoenergetic. Given the rates of photoinitiated electron transfer observed in the other diporphyrin systems to be discussed below, where the thermodynamic driving force is much greater, the lack of electron transfer is not unexpected.

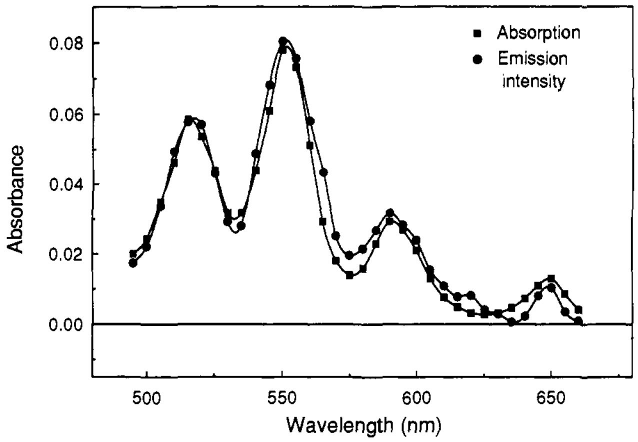

Figure 3. Absorption and corrected fluorescence excitation spectra for diporphyrin **4** in dichloromethane solution. The fluorescence was monitored at 720 nm, where only the free base porphyrin moiety emits significantly. The spectra have been normalized in the 510–520-nm region, where most of the absorption is due to the free base porphyrin. The spectra are essentially identical throughout their range, indicating that singlet–singlet energy transfer is virtually complete.

Scheme III

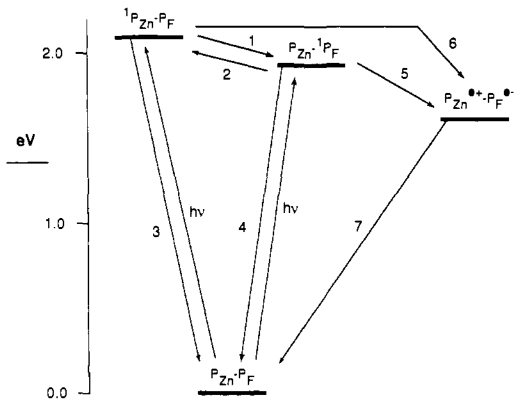

There is a reasonable driving force (0.19 eV) for electron transfer from the zinc porphyrin first excited singlet state to yield $P_{Zn}^{\bullet+}$–$P^{\bullet-}$ (Table I). However, fluorescence excitation experiments reveal that singlet–singlet energy transfer from the zinc porphyrin to the free base moiety is essentially quantitative (Figure 3). Thus, energy transfer is much more rapid than electron transfer in this system, and the quantum yield of electron transfer from $^1P_{Zn}$–P is essentially zero. Again, as will be discussed below, this is not unexpected.

Diporphyrin 7. The structure of this dyad resembles that of **4**, but the zinc porphyrin now carries three *p*-tolyl groups, whereas the free base porphyrin bears three pentafluorophenyl moieties. The fluorinated species are strongly electron withdrawing and therefore stabilize a negative charge on the attached porphyrin. As a result, the energetics for **7**, estimated from spectrophotometric and cyclic voltammetric data (Table I), are as depicted in Scheme III. Electron transfer either from the zinc porphyrin first excited singlet state or to the free base porphyrin first excited singlet state is exergonic, and one might therefore expect to observe photoinitiated electron transfer in this molecule.

The absorption spectrum of **7** in dichloromethane solution is a linear combination of those of the unlinked model compounds **10** and **11**, with Q-band maxima at 510, 550, 588, and 640 nm and a Soret absorption at 422 nm. In emission, the model metalated porphyrin **10** has maxima as shown in Figure 1, whereas the model free base **11** has maxima at 643 and 713 nm in a ratio of 1:2.5, respectively. The emission of the dyad **7** with excitation at 550 nm features maxima at 600, 643, and 710 nm in a ratio of 1.0:4.6:10.0. The small band at 600 nm is characteristic of emission from the zinc porphyrin moiety, whereas the other two bands arise mainly from the free base porphyrin moiety. The low intensity of the zinc porphyrin emission suggests that the zinc porphyrin first excited singlet state is being strongly quenched.

---

[28] Possible impurities include certain metalated porphyrins (*e.g.*, zinc) and diprotonated porphyrins, which have first excited singlet state lifetimes of *ca.* 1.5 ns. Alternatively, the 1.5-ns component could be accommodated by a kinetic analysis in which P_{Zn}–^1P is in equilibrium with a $P_{Zn}^{\bullet+}$–$P^{\bullet-}$ charge-separated state (see Scheme II). However, this rationalization requires rather unlikely values for the various electron-transfer rate constants, based on the rates observed for the other molecules in this series.

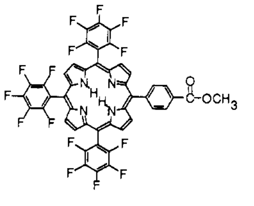

11

Time-resolved fluorescence studies shed some light on the nature of this quenching. Fluorescence from a dichloromethane solution of **7** excited at 590 nm was monitored at seven wavelengths in the 640–725-nm region. The seven resulting decays were analyzed simultaneously to give a global fit to two exponentials with a χ^2 of 1.11 (Figure 4). The two components had lifetimes of 82 ps and 2.7 ns, respectively. The shorter component had a positive amplitude in the 640–670-nm region, where the zinc porphyrin moiety emits strongly, and a negative amplitude in the 700–725-nm region, where the emission is due mainly to the free base porphyrin. Thus, as was the case with **4**, the short component is associated with singlet–singlet energy transfer from the metalated to the free base moiety, and the lifetime of the zinc porphyrin first excited singlet state is 82 ps. The lifetime of the first excited singlet state of model zinc porphyrin **10** is 1.6 ns.

There are two reasonable explanations for the quenching of the zinc porphyrin first excited singlet state. The first is energy transfer (step 1 in Scheme III) as discussed above. The time-resolved fluorescence studies reveal that this does indeed occur. However, Scheme III suggests that electron transfer from the zinc porphyrin first excited singlet state to yield $P_{Zn}^{\bullet+}-P_F^{\bullet-}$ (step 6 in the scheme) is exergonic by 0.48 eV and therefore should be considered as well. This possibility was investigated by using steady-state fluorescence excitation spectroscopy. Figure 5 shows the corrected excitation spectrum of **7** in dichloromethane with emission at 720 nm, where only the free base porphyrin emits significantly. The spectrum has been normalized to the absorption spectrum of **7** in the 500–510- and 640-nm regions, where absorption is due almost entirely to the free base porphyrin. It is evident that the corrected excitation spectrum is significantly lower than the absorption spectrum in the 550- and 590-nm regions, where the zinc porphyrin moiety absorbs strongly. Thus, energy transfer is not complete. Quantitatively, estimation of the singlet–singlet energy transfer quantum yield at 550 and 590 nm gives 0.74 and 0.79, respectively. Thus, the quantum yield of singlet energy transfer (step 1 in Scheme III) is taken to be about 0.77 in **7**. Given this number and the 82-ps lifetime for the zinc porphyrin first excited singlet state, eq 2 may be used to calculate the singlet–singlet energy-transfer rate constant k_1 to be 9.4×10^9 s^{-1}.

Scheme III and Table I show that the excited singlet states $^1P_{Zn}-P_F$ and $P_{Zn}-{}^1P_F$ differ in energy by 0.16 eV. The equilibrium constant for energy transfer is thus 510 at 298 K (eq 3), and the rate of energy transfer from the free base porphyrin moiety to the zinc porphyrin (k_2) is therefore 1.8×10^7 s^{-1}.

Turning now to electron transfer, because the repopulation of $^1P_{Zn}-P_F$ via step 2 is negligible, the lifetime of the zinc porphyrin first excited singlet state is given by

$$\frac{1}{\tau} = k_1 + k_3 + k_6 \tag{4}$$

The value of k_1 was given above, and that of k_3 may be estimated as 6.3×10^8 s^{-1} from the 1.6-ns fluorescence lifetime of model porphyrin **10**, which cannot undergo energy or electron transfer. Thus, by eq 4, the electron-transfer rate constant k_6 is 2.2×10^9 s^{-1}. The quantum yield of $P_{Zn}^{\bullet+}-P_F^{\bullet-}$ from $^1P_{Zn}-P_F$ via step 6, calculated with eq 2, is 0.18.

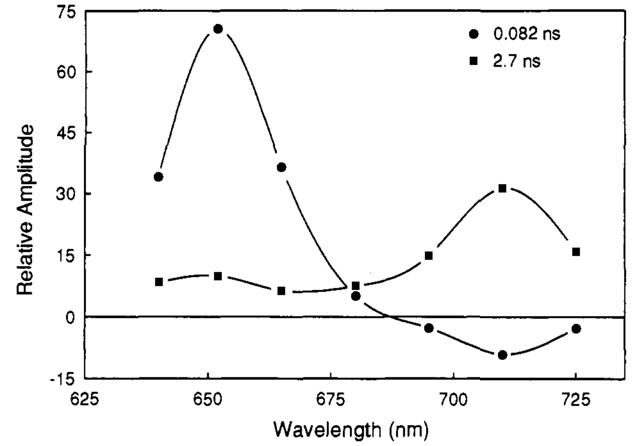

Figure 4. Decay-associated spectra for diporphyrin **7** in dichloromethane solution with excitation at 590 nm. The two components of the decay were determined by a global analysis of decays taken at the seven indicated wavelengths (global $\chi^2 = 1.11$).

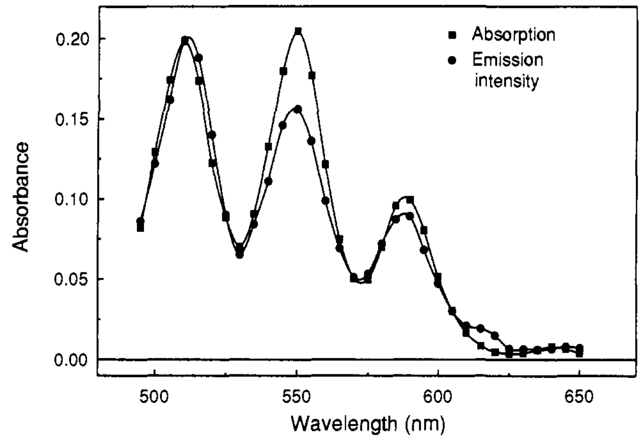

Figure 5. Absorption and corrected fluorescence excitation spectra for diporphyrin **7** in dichloromethane solution. The fluorescence was monitored at 720 nm, where only the free base porphyrin moiety emits significantly. The spectra have been normalized in the 500–510- and 640-nm regions, where most of the absorption is due to the free base porphyrin. The fact that the spectra are not identical in regions where the zinc porphyrin moiety absorbs strongly indicates that singlet–singlet energy transfer is incomplete.

The longer lived component of the fluorescence decay of **7** (2.7 ns, Figure 4) has the spectrum of the free base porphyrin moiety and therefore represents the decay of $P_{Zn}-{}^1P_F$. Two of the possibilities for decay of this excited singlet state are singlet–singlet energy transfer as discussed above via step 2 in Scheme III and decay via the usual photophysical processes (lumped together as step 4 in the scheme). The above analysis shows that the energy-transfer route may be ignored. In addition, the rate constant for step 4 may be estimated as 1.2×10^8 s^{-1} from the 8.5-ns singlet excited state lifetime measured for model porphyrin **11**. Thus, neither steps 2 nor 4 can explain the relatively short lifetime of $P_{Zn}-{}^1P_F$, and another quenching process must be occurring. Scheme III suggests that this is electron transfer from the adjacent zinc porphyrin to yield $P_{Zn}^{\bullet+}-P_F^{\bullet-}$ (step 5). According to the scheme, this process should be exergonic by about 0.32 eV. This being the case, the electron-transfer rate constant k_5 may be estimated from

$$k_5 = \frac{1}{\tau} - \frac{1}{\tau_0} \tag{5}$$

where τ is the 2.7-ns component of the fluorescence decay of **7** and τ_0 is the 8.5-ns lifetime of **11**. The electron-transfer rate constant calculated in this way is 2.5×10^8 s^{-1}. The quantum yield of electron transfer ϕ_5, is τk_5, or 0.68, based upon $P_{Zn}-{}^1P_F$.

Carotenodiporphyrin Triad 1. The time-resolved fluorescence data for **7** suggest that when sufficient thermodynamic driving force exists, interporphyrin electron transfer in P_A-P_B dyads can compete with the other pathways that relax the porphyrin first excited singlet states to generate $P_A^{\bullet+}-P_B^{\bullet-}$. Our experience with other multicomponent molecular devices[3,17] suggests that if this is the case, incorporation of a suitable diporphyrin moiety into a triad of the type $C-P_A-P_B$ might well lead to a long-lived

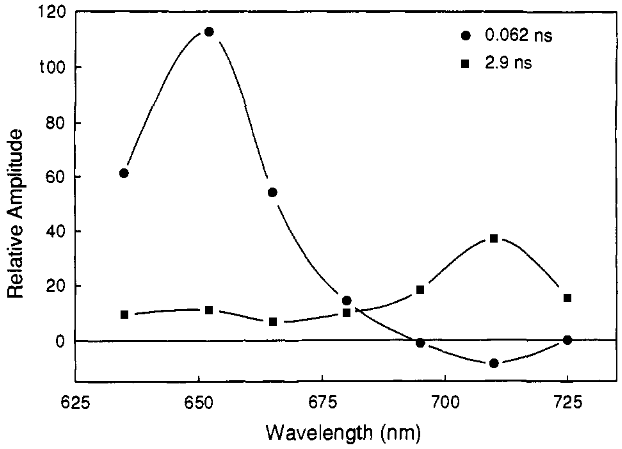

Figure 6. Decay-associated spectra for carotenodiporphyrin triad **1** in dichloromethane solution with excitation at 590 nm. The two components of the decay were determined by a global analysis of decays taken at the seven indicated wavelengths (global $\chi^2 = 1.13$).

charge-separated state ($C^{\bullet+}$–P_A–$P_B^{\bullet-}$) via secondary electron transfer from the carotenoid polyene. Triad **1** was prepared with this possibility in mind.

The absorption spectrum of **1** is nearly identical with a linear combination of the spectra of model compounds **11** and **12**. The Soret band appears at 422 nm, and three porphyrin Q-bands are found at 550, 588, and 640 nm. The shorter wavelength Q-bands are obscured by the absorption of the carotenoid moiety, which has maxima at 482 and 508 nm. Again, there is no evidence in the absorption spectrum for strong interactions among the various components as a result of their linkage, and the three moieties behave in absorption essentially as isolated chromophores.

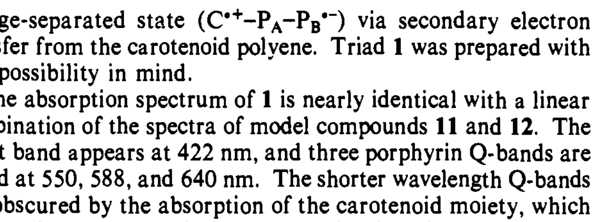
12

The corrected fluorescence emission spectrum of **1** in dichloromethane solution with excitation at 425 nm is similar to that of the model free base **11**, with maxima at 641 and 709 nm in a ratio of 1:2.6. There is only a trace of emission from the zinc porphyrin moiety at 600 nm, and carotenoids of the type employed in **1** are essentially nonfluorescent. By analogy with the results for **7**, a combination of singlet–singlet energy transfer and photoinduced electron transfer from the zinc porphyrin to the free base may be invoked to rationalize this result.

Time-resolved emission experiments helped confirm this conclusion. A solution of **1** in dichloromethane was excited at 590 nm, and emission decays were measured at seven wavelengths in the 635–725-nm region. Global analysis of the seven decays required two exponential components with lifetimes of 62 ps and 2.9 ns, with a global χ^2 value of 1.13. The results are shown in Figure 6. As was the case for **7**, the 62-ps component makes a large positive contribution to the decay in the 640–650-nm region, where zinc porphyrin emission is strong, and a negative contribution around 710 nm, where the free base porphyrin emits. This result is consistent with singlet–singlet energy transfer from $C{-}^1P_{Zn}{-}P_F$ to yield $C{-}P_{Zn}{-}^1P_F$. This process is shown as step 1 in Scheme IV, which depicts the various high-energy states of **1** and some of the pathways by which they may interconvert. The energetics shown in the scheme are derived from appropriate model compounds (Table I).

In order to understand the decay kinetics for **1**, data for model compounds **11** and **12** are necessary. As discussed above, **11** has a fluorescence lifetime of 8.5 ns. Excitation of a dichloromethane solution of carotenoporphyrin **12** at 591 nm resulted in the observation of a decay at 610 nm, which was satisfactorily fit as two exponential components of 0.31 ns (97% of the decay) and 1.2 ns (3% of the decay). The major component represents decay of $C{-}^1P_{Zn}$, whereas the minor contributor may be due to a small amount of impurity in which the carotenoid has been destroyed. The short lifetime of this porphyrin moiety relative to that of molecule **10**, which lacks the carotenoid, is consistent with observations for other carotenoporphyrin species.[29] The nature of this quenching process is unknown, and several possible mechanisms have been suggested. One of these involves photoinduced electron transfer to form $C^{\bullet+}{-}P^{\bullet-}$. If such a state were indeed formed, it could in principle contribute to the formation of long-lived charge-separated states (see below). However, attempts to associate such quenching with intramolecular electron transfer have been unsuccessful to date.[29]

Scheme IV

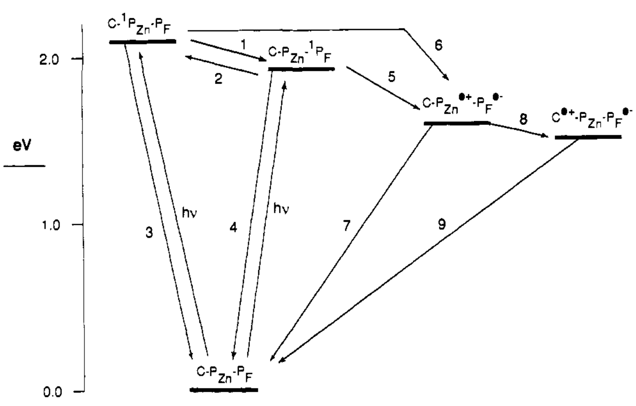

Scheme IV suggests that $C{-}^1P_{Zn}{-}P_F$ in **1** can decay by three pathways (steps 1, 3, and 6). The results for **12** allow us to estimate a value of $3.2 \times 10^9\ s^{-1}$ for k_3. The singlet–singlet energy-transfer quantum yield for **1** is difficult to determine by fluorescence excitation studies because of interference by carotenoid absorptions. However, the singlet–singlet energy transfer rate constants k_1 and k_2 are expected to be virtually identical for dyad **7** and triad **1**, as the first excited singlet state energies and diporphyrin moieties are nearly identical. Thus, we assign $k_1 = 9.4 \times 10^9\ s^{-1}$. The quantum yield of singlet–singlet energy transfer, by eq 2, is 0.58.

The rate constant for electron transfer from the zinc porphyrin first excited singlet state to yield $C{-}P_{Zn}^{\bullet+}{-}P_F^{\bullet-}$ by step 6 in Scheme IV may be estimated with use of eq 4. The 62-ps lifetime for $C{-}^1P_{Zn}{-}P_F$ and the values for k_1 and k_3 mentioned above yield $k_6 = 3.5 \times 10^9\ s^{-1}$. This value is very close to that found for the similar electron-transfer step in dyad **7**. The electron-transfer quantum yield of step 6 based on $C{-}^1P_{Zn}{-}P_F$ is 0.22.

As was the case for **7**, the lifetime of the free base porphyrin first excited singlet state of **1** is shortened from its normal value of 8.5 ns due to electron transfer to form, in this case, $C{-}P_{Zn}^{\bullet+}{-}P_F^{\bullet-}$ (step 5 in Scheme IV). The rate constant for this step, calculated with use of eq 4 from the 2.9-ns component of the fluorescence decay, is $2.3 \times 10^8\ s^{-1}$. Within experimental error, this value is identical with that found for **7** ($2.5 \times 10^8\ s^{-1}$). The quantum yield of $C{-}P_{Zn}^{\bullet+}{-}P_F^{\bullet-}$ based upon $C{-}P_{Zn}{-}^1P_F$ is given by τk_5 and equals $(2.9 \times 10^{-9})(2.3 \times 10^8)$, or 0.67.

It is clear from the above discussion that the initial charge-separated state $C{-}P_{Zn}^{\bullet+}{-}P_F^{\bullet-}$ in **1** is formed by two routes, steps 5 and 6 in Scheme IV. The overall quantum yield of this state will vary depending upon excitation wavelength. Most of the time-resolved fluorescence and absorption (see below) studies have been performed with 590-nm excitation. Ignoring a minor contribution from the carotenoid polyene, approximately 47% of the light at this wavelength is absorbed by the zinc porphyrin moiety and 53% by the free base. The quantum yield of $C{-}P_{Zn}^{\bullet+}{-}P_F^{\bullet-}$ via step 6 in Scheme IV, based on total light absorbed at 590 nm,

---

(29) Moore, T. A.; Gust, D.; Hatlevig, S.; Moore, A. L.; Makings, L. R.; Pessiki, P. J.; DeSchryver, F. S.; Van der Auweraer, M.; Lexa, D.; Bensasson, R. V.; Rougée, M. *Isr. J. Chem.* **1988**, *28*, 87 and references cited therein.

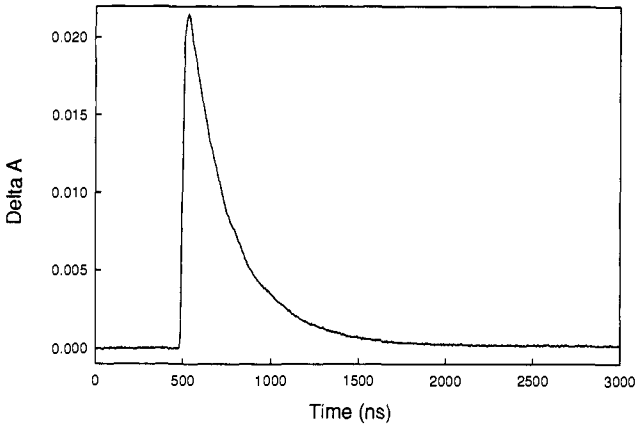

Figure 7. Decay of the carotenoid radical cation absorption of $C^{\bullet+}$–P_{Zn}–$P_F^{\bullet-}$ formed by excitation of a dichloromethane solution of carotenodiporphyrin triad **1** with a 590-nm, ca. 15-ns laser pulse. A three-parameter (floating base line) fit of the data yields a single exponential decay with a lifetime of 240 ns.

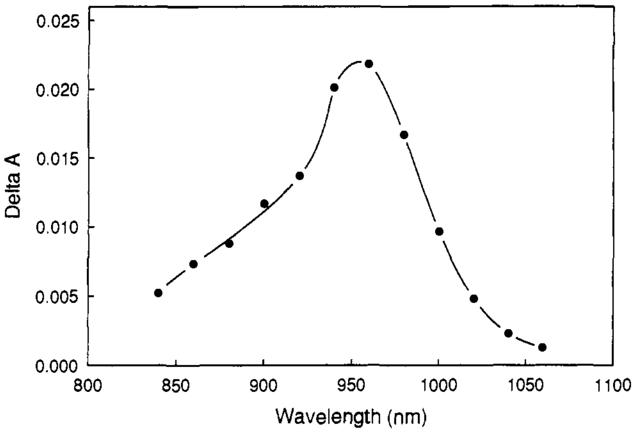

Figure 8. Spectrum of the transient absorption of $C^{\bullet+}$–P_{Zn}–$P_B^{\bullet-}$ shown in Figure 7. This spectrum, taken 10 ns after the excitation flash, is characteristic of the carotenoid radical cation.

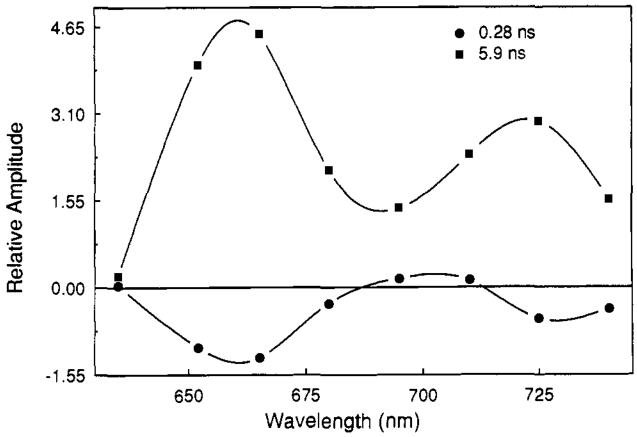

Figure 9. Decay-associated spectra for diporphyrin **5** in dichloromethane solution with excitation at 590 nm. The two components of the decay were determined by a global analysis of decays taken at the eight indicated wavelengths (global χ^2 = 1.09).

Scheme V

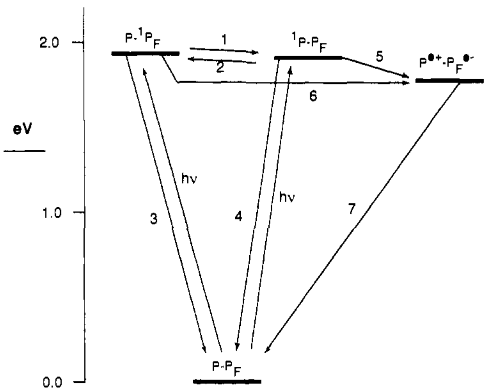

is therefore 0.47 × 0.22 = 0.10. The quantum yield via step 5 from light directly absorbed by the free base porphyrin is 0.53 × 0.67 = 0.36, and that from light absorbed by the zinc porphyrin moiety and transferred to the free base is 0.47 × 0.58 × 0.67 = 0.18. Thus, the quantum yield of C–$P_{Zn}^{\bullet+}$–$P_F^{\bullet-}$ via all pathways and based upon total light absorbed by the two porphyrins at 590 nm is 0.64.

Scheme IV suggests that formation of C–$P_{Zn}^{\bullet+}$–$P_F^{\bullet-}$ might be followed by a secondary electron transfer from the carotenoid to the zinc porphyrin radical cation (step 8) to yield a final $C^{\bullet+}$–P_{Zn}–$P_F^{\bullet-}$ state. Transient absorption studies on the nanosecond time scale reveal that such a state is in fact produced. Irradiation of a dichloromethane solution of **1** with a 590-nm, ca. 15-ns laser pulse resulted in the observation of a transient absorption in the 960-nm region, which decayed exponentially with a lifetime of 240 ns (Figure 7). The spectrum of this transient (Figure 8) reveals that it is due to a carotenoid radical cation.[30] Thus, the transient is ascribed to the species $C^{\bullet+}$–P_{Zn}–$P_F^{\bullet-}$. The quantum yield, calculated by the comparative method[31] and based upon the total light absorbed at 590 nm, is 0.32.

Diporphyrin 5. Dyad **5** is a close relative of **7** in which both porphyrin moieties are present in the free base form. As a result, the two first excited singlet states are nearly isoenergetic. The first excited singlet state of model porphyrin **8** lies at 1.90 eV, whereas that of **11** is at 1.93 eV. The lowest energy charge-separated state $P^{\bullet+}$–$P_F^{\bullet-}$ is at 1.77 eV (Table I). Thus, electron transfer from either excited singlet state is energetically possible (Scheme V).

Spectroscopic studies of **5** were undertaken in order to investigate this possibility. The absorption spectrum in dichloromethane solution is a linear combination of those of model compounds **8** and **11**. The corrected fluorescence emission spectrum with excitation at 590 nm features maxima at 655 and 718 nm in a ratio of 1.5:1.

Time-resolved emission studies in dichloromethane with excitation at 590 nm were performed at eight wavelengths in the 635–718-nm region. A global analysis of the resulting decays yielded a good fit to two exponential functions with χ^2 = 1.09 (Figure 9). The first component of the decay has a lifetime of 0.28 ns and reflects a growth in fluorescence emission in the 660- and 725-nm regions and a decay in the 700–710-nm region, where the fluorinated porphyrin contributes most strongly to the decay. Thus, this component is associated with energy transfer from P–^1P_F to yield ^1P–P_F. The longer lived component of the decay, whose emission spectrum resembles that of ^1P–P_F, has a lifetime of 5.9 ns.

The time-resolved data may be discussed in terms of Scheme V. The difference in energies of the two porphyrin first excited singlet states is only 0.03 eV. Thus, the equilibrium constant (K) for singlet–singlet energy transfer is 3.2 at ambient temperatures. If singlet–singlet energy transfer (steps 1 and 2) occurs at rates comparable to or greater than those of the other steps shown in the scheme, both excited singlet states will be significantly populated during the decay process and the kinetic analysis will be more complicated than that used for **7** above. The general solution for coupled reactions of this type[32] reveals that two fluorescence lifetimes (τ_1 and τ_2) are to be expected for the decay of the two

---

[30] Land, E. J.; Lexa, D.; Bensasson, R. V.; Gust, D.; Moore, T. A.; Moore, A. L.; Liddell, P. A.; Nemeth, G. A. *J. Phys. Chem.* **1987**, *91*, 4831.

[31] Bensasson, R.; Goldschmidt, C. R.; Land, E. J.; Truscott, T. G. *Photochem. Photobiol.* **1978**, *28*, 277.

[32] Demas, J. N. *Excited State Lifetime Measurements*; Academic Press: New York, 1983; p 59.

excited singlet states. The reciprocals of these lifetimes (γ_1 and γ_2) do not in general represent any of the rate constants in the scheme. Rather

$$\gamma_1 = \{(X + Y) + [(X - Y)^2 + 4k_1k_2]^{1/2}\}/2 \qquad (6)$$

$$\gamma_2 = \{(X + Y) - [(X - Y)^2 + 4k_1k_2]^{1/2}\}/2 \qquad (7)$$

where

$$X = k_3 + k_6 + k_1 \qquad (8)$$

$$Y = k_4 + k_5 + k_2 \qquad (9)$$

The quantities γ_1 and γ_2 are known from the fluorescence decay results, and k_3 and k_4 may be estimated to be 1.2×10^8 and 1.3×10^8 s^{-1} from the fluorescence lifetimes of model compounds **8** and **11**, respectively. The equilibrium constant for singlet energy transfer K gives k_2 as $k_1/3.2$. Thus, one is left with two equations (6 and 7) and three unknowns (k_1, k_5, and k_6). Setting $k_6 = Bk_5$ allows one to work out an analytical solution to eqs 6 and 7 in quadratic form:

$$k_2 = \frac{-b \pm (b^2 - 4ac)^{1/2}}{2a} \qquad (10)$$

where

$$a = 4[(K - B)^2 + (B + 1)^2K] \qquad (11)$$

$$b = 4(K - B)[(B - 1)(\gamma_1 + \gamma_2) + 2(k_3 - Bk_4)] \qquad (12)$$

$$c = [(B - 1)(\gamma_1 + \gamma_2) + 2(k_3 - Bk_4)]^2 - (B + 1)^2(\gamma_1 - \gamma_2)^2 \qquad (13)$$

Equation 10 may thus be solved for different values of B, and the resulting k_2 values may be used in conjunction with eqs 6–9 to determine k_1, k_5, and k_6. Maximum values for k_5 and k_6 of 5.5×10^7 and 1.8×10^8 s^{-1}, respectively, may be calculated by setting the complementary rate constant to zero. The k_1 and k_2 values are essentially independent of B, with $k_1 = 2.6 \times 10^9$ s^{-1} and $k_2 = 8.1 \times 10^8$ s^{-1}.

The small difference in thermodynamic driving force for steps 5 and 6, coupled with the fact that both electron-transfer reactions occur in the same molecule and from closely related chromophores to yield the same charge-separated state suggests that the approximation that $k_5 = k_6$ may be a useful one. If this assumption is made, the above equations yield $k_5 = k_6 = 4.1 \times 10^7$ s^{-1}. This value appears reasonable, when one considers that the thermodynamic driving force difference between steps 6 and 5 in dyad **7** (0.16 eV) is identical with that between step 5 in dyad **7** and step 6 in dyad **5**. If one assumes that the dependence of the natural logarithm of the electron-transfer rate constant on energy gap is roughly linear in this region, then the ratio of k_6 to k_5 in **7** (8.8) suggests that k_6 in **5** should be about 3.6×10^7 s^{-1}, which is rather close to that calculated above. Of course, the assumption that $k_5 = k_6$ in dyad **5** ignores the potentially significant fact that whereas the excited porphyrin is the electron *acceptor* in step 6, it is the electron *donor* in step 5.

Carotenodiporphyrin Triad 2. The observation of fluorescence quenching in dyad **5**, ascribed to photoinitiated electron transfer, coupled with the long-lived $C^{\bullet+}$–P_{Zn}–$P_F^{\bullet-}$ charge-separated state detected for triad **1** suggests that a similar long-lived state might be formed in triad **2**, which features both porphyrins in the free base form. The absorption spectrum of **2** in dichloromethane is nearly identical with a linear combination of those of model porphyrin **11** and carotenoporphyrin **13**. The emission spectrum in the same solvent with excitation at 590 nm is similar to that of related dyad **5**, with maxima at 656 and 718 nm, in a ratio of intensities of 1.7:1.

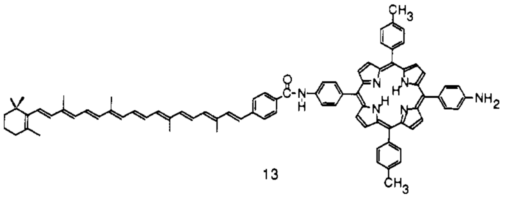

13

Scheme VI

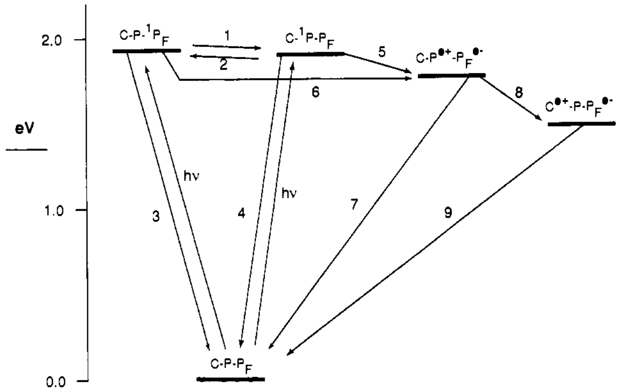

Time-resolved emission studies in dichloromethane were performed at nine wavelengths in the 640–730-nm region, with excitation at 590 nm. A global analysis of the decays yielded a good fit to three exponential components with $\chi^2 = 1.08$. Two decays of 0.25 and 2.9 ns arise from **2**, whereas a minor 5.5-ns component likely represents an impurity.

Turning to Scheme VI, it is evident that the porphyrin energetics for **2** closely resemble those for **5**, with the C–^{1}P–P$_F$ and C–P–^{1}P$_F$ states at 1.90 and 1.93 eV, respectively, and a possible C–P$^{\bullet+}$–P$_F^{\bullet-}$ charge-separated state at 1.77 eV. Therefore, the time-resolved fluorescence results may be analyzed as described above with eqs 6–13 and a value of $k_4 = 2.9 \times 10^8$ s^{-1} from model carotenoporphyrin **13**. The values of k_3 and the equilibrium constant K are identical with those for **5**. If one again assumes that $k_5 = k_6$ in Scheme VI, then the equations yield $k_1 = 2.9 \times 10^9$ s^{-1}, $k_2 = 8.9 \times 10^8$ s^{-1}, and $k_5 = k_6 = 9.7 \times 10^7$ s^{-1}. These results are relatively close to those found for **5**, as might be expected, given the similarities between the two molecules.

Transient absorption studies on the nanosecond time scale were undertaken in order to detect any formation of C$^{\bullet+}$–P–P$_F^{\bullet-}$ via step 8 in Scheme VI. Indeed, excitation of a dicholoromethane solution of **2** at 590 nm resulted in the observation of a transient carotenoid radical cation absorption due to C$^{\bullet+}$–P–P$_F^{\bullet-}$, which is formed with a quantum yield of 0.19, based upon total light absorbed. The charge-separated state decayed with a lifetime of 250 ns.

Conclusions

The steady-state and time-resolved fluorescence data for the porphyrin dyads discussed above clearly demonstrate that singlet–singlet energy transfer between the porphyrin moieties is facile and that the linking of the porphyrins has opened up new pathways, ascribed to electron transfer, for decay of the porphyrin excited singlet states. The fact that this new quenching is only observed in the dyads in which a charge-separated state lies at a lower energy than one or both of the first excited singlet states strongly supports the assignment of the quenching process to electron transfer, rather than to some other photophysical or photochemical process.[33] The assignment is verified by triads **1** and **2**, in which the initially produced charge-transfer state is trapped to yield a long-lived, energetic charge-separated state of the form C$^{\bullet+}$–P–P$^{\bullet-}$. The singlet–singlet energy and electron-transfer rate constants determined in this research are summarized in Table II.

Singlet–Singlet Energy Transfer. With regard to singlet–singlet energy transfer, it is evident that the rate constant k_1 changes as the energies of the two porphyrin first excited singlet states and therefore their absorption and emission spectra change. Singlet–singlet energy transfer between porphyrin moieties is often discussed in terms of the Förster equation,[34–36] which states that

$$k_{ss} = \frac{9(\ln 10)\kappa^2}{128\pi^5 n^4 N' \tau_D{}^\circ R^6} \int f_D(\nu)\epsilon_A(\nu)\nu^{-4}\,d\nu \qquad (14)$$

---

(33) Wasielewski, M. R.; Johnson, D. G.; Niemczyk, M. P.; Gaines, G. L., III; O'Neil, M. P.; Svec, W. A. *J. Am. Chem. Soc.* **1990**, *112*, 6482.

Table II. Rate Constants (s^{-1}) and Free Energy Change (eV) for Singlet–Singlet Energy and Electron Transfer in Diporphyrins and Carotenodiporphyrins at 298 K

compd	k_1 ($\Delta G°$)	k_2 ($\Delta G°$)	k_5 ($\Delta G°$)	k_6 ($\Delta G°$)
1[a]	9.4×10^9 (−0.16)	1.8×10^7 (0.16)	2.3×10^8 (−0.32)	3.5×10^9 (−0.48)
2[b]	2.9×10^9 (−0.03)	8.9×10^8 (0.03)	9.7×10^7 (−0.13)	9.7×10^7 (−0.16)
4	2.3×10^{10} (−0.18)	2.1×10^7 (0.18)		
5[b]	2.6×10^9 (−0.03)	8.1×10^8 (0.03)	4.1×10^7 (−0.13)	4.1×10^7 (−0.16)
7	9.4×10^9 (−0.16)	1.8×10^7 (0.16)	2.5×10^8 (−0.32)	2.2×10^9 (−0.48)

[a] Values for k_1 and k_2 were estimated from the results for **7**. [b] Assuming $k_5 = k_6$ (see text).

In this equation, k_{ss} is the singlet–singlet energy transfer rate constant, κ^2 is a function of the relative orientation of the transition dipole moments (see below), n is the index of refraction of the solvent, N' is the number of molecules per millimole (Avogadro's constant × 10^{-3}), $\tau_D°$ is the natural fluorescence lifetime of the excited donor (the reciprocal of the radiative rate constant), and R (cm) is the distance between the centers of the two dipoles in question. The integral represents the overlap between the donor emission spectrum and the acceptor absorption spectrum, where ϵ_A (cm^2/mmol (=L/mol·cm)) is the molar decadic extinction coefficient of the acceptor and ν is in inverse centimeters. The appropriate units for the overlap integral are centimeters to the sixth power per millimole. The value of $\tau_D°$ may be calculated from

$$\tau_D = \Phi_D^f \tau_D° \qquad (15)$$

where τ_D is the lifetime of the first excited singlet state of the donor in the absence of energy- or electron-transfer processes and Φ_D^f is the corresponding fluorescence quantum yield.

Equation 14 was applied to diporphyrin **4**, with use of $n = 1.425$ for dichloromethane, $\Phi_D^f = 0.03$ (from that for zinc *meso*-tetraphenylporphyrin),[26] $\tau_D = 1.6 \times 10^{-9}$ s^{-1} (from **10**), and $R = 1.87 \times 10^{-7}$ cm (estimated from molecular models). The value of the overlap integral was 2.78×10^{-14} cm^6/mmol. This value is similar to those calculated for other P_{Zn}–P diporphyrin systems.[37,38]

The orientation factor κ^2 depends upon the angle between the transition dipoles. It is given by

$$\kappa^2 = (\cos\gamma - 3\cos\alpha\cos\beta)^2 \qquad (16)$$

where α and β are the angles that the transition dipoles make with a line joining their centers and γ is the angle between the two transition dipoles. In the case of the diporphyrin systems, α and β are both approximately 45°. The angle γ also depends upon the dihedral angle between the porphyrin planes. This dihedral angle is unknown but must lie between 0 and 90°. These two values give limiting values for κ^2 of 0.25 and 2.25.

Equation 14 yields values for the singlet–singlet energy-transfer rate constant k_{ss} in **4** of 6.5×10^8 s^{-1} for the minimum value of κ^2 and 5.9×10^9 s^{-1} for the maximum. The average value of κ^2 for a random distribution of orientations is $^2/_3$, and this in turn gives $k_{ss} = 1.7 \times 10^9$ s^{-1}. The measured value of k_1 is 2.3×10^{10} s^{-1}.

Similar calculations were carried out for diporphyrins **5** and **7**. In the case of **5**, the k_{ss} values for $\kappa^2 = 0.25$, 0.667, and 2.25 were 4.8×10^8, 1.3×10^9, and 4.3×10^9 s^{-1}, whereas a value of 2.6×10^9 s^{-1} was found experimentally. For **7**, the corresponding calculated values were 4.6×10^7, 1.2×10^8, and 4.1×10^8 s^{-1}, respectively. The lower values are due to the fact that less favorable overlap between the donor emission and acceptor absorption reduces the overlap integral to 1.88×10^{-15} cm^6/mmol. The experimentally measured value of k_1 was 9.4×10^9 s^{-1}.

The singlet–singlet energy-transfer rate constants determined experimentally and reported in Table II are fairly similar to those reported for other covalently linked porphyrin dyads and related materials,[37-41] but quantitative comparisons are of little value because of structural differences and because of conformational heterogeneity in some of the previously studied molecules.

On the other hand, comparison of the experimental results with those calculated with the Förster equation reveals some interesting discrepancies. The experimentally derived singlet–singlet energy-transfer rate constant for metal-free diporphyrin **5** falls well within the range of values predicted by the Förster treatment ($k_{ss} = 1.3 \times 10^9$ s^{-1} for a random distribution; $k_1 = 2.6 \times 10^9$ s^{-1}). In the zinc analogue **7**, the measured rate (9.4×10^9 s^{-1}) is ~80 times faster than that calculated for a random distribution. The zinc-containing diporphyrin **4** was found to have a measured rate 14 times that calculated for a random distribution. The failure of the Förster formulation for the zinc species suggests that mechanisms involving stronger coupling are contributing to energy transfer. The observation of photoinitiated electron transfer in **1**, **2**, **5**, and **7** demonstrates that electron exchange interactions are present in these molecules, and it is likely that these interactions lead to significant singlet–singlet energy-transfer rate constants.[42]

Electron Transfer. With respect to photoinitiated electron transfer, inspection of Table II shows that, in these systems, the electron-transfer rate constant increases with the energy gap. Although too few data points are available to permit meaningful fitting of the rate constant vs energy gap data to electron-transfer theories such as that of Marcus,[43] it is clear that, up to a thermodynamic driving force of 0.48 eV, there is no evidence for any inverted behavior, or lack of dependence upon energy gap. In terms of the Marcus equation, the reorganization energy (λ) must be greater than or equal to 0.5 eV in these systems.

In the C–P–P triad molecules, the rate constants for steps 7 (charge recombination of the $C\text{–}P^{\bullet+}\text{–}P^{\bullet-}$ state) and 8 (electron transfer from the carotenoid to produce $C^{\bullet+}\text{–}P\text{–}P^{\bullet-}$) are of particular interest because their ratio helps control the quantum yield of the final $C^{\bullet+}\text{–}P\text{–}P^{\bullet-}$ state. Direct information concerning the rates of these steps must await transient absorption experiments on the picosecond time scale. However, some information is available from the quantum yield data. In triad **1**, the quantum yield of $C\text{–}P_{Zn}{}^{\bullet+}\text{–}P_F{}^{\bullet-}$ is 0.64 with excitation at 590 nm, based upon total light absorbed by the two porphyrin moieties, whereas the overall quantum yield of $C^{\bullet+}\text{–}P_{Zn}\text{–}P_F{}^{\bullet-}$ is 0.32. Thus, the efficiency of step 8 is about 50%. This is substantially higher than that found for a related step in a number of carotenoporphyrin–quinone (C–P–Q) triad molecules.[3,29,44] In carotenodiporphyrin triad **2**, the efficiency of step 8 would be expected to be even greater. The lack of a zinc ion in P raises the energy of $C\text{–}P^{\bullet+}\text{–}P_F{}^{\bullet-}$

---

(34) Förster, T. *Ann. Phys. (Leipzig)* **1948**, *2*, 55.

(35) Förster, T. *Discuss. Faraday Trans.* **1965**, *27*, 7.

(36) Eyring, H.; Lin, S. H.; Lin, S. M. *Basic Chemical Kinetics*; John Wiley & Sons: New York, 1980; pp 289–297.

(37) Brookfield, R. L.; Henriette, E.; Harriman, A.; Porter, G. *J. Chem. Soc., Faraday Trans.* **1986**, *82*, 219.

(38) Anton, J. A.; Loach, P. A.; Govindjee *Photochem. Photobiol.* **1978**, *28*, 235.

(39) Osuka, A.; Maruyama, K.; Yamazaki, I.; Tamai, N. *J. Chem. Soc., Chem. Commun.* **1988**, 1243.

(40) Tran-Thi, T. H.; Desforge, C.; Thiec, C.; Gaspard, S. *J. Phys. Chem.* **1989**, *93*, 1226.

(41) Rempel, U.; von Maltzan, B.; von Borczyskowski, C. *Chem. Phys. Lett.* **1990**, *169*, 347.

(42) For some other systems in which singlet–singlet energy transfer via an exchange mechanism has been proposed, see: Moore, A. L.; Dirks, G.; Gust, D.; Moore, T. A. *Photochem. Photobiol.* **1980**, *32*, 691. Zimmerman, H. E.; Goldman, T. D.; Hirzel, T. K.; Schmidt, S. P. *J. Org. Chem.* **1980**, *45*, 3933. Kroon, J.; Oliver, A. M.; Paddon-Row, M. N.; Verhoeven, J. W. *J. Am. Chem. Soc.* **1990**, *112*, 4868.

(43) Marcus, R. A. *J. Chem. Phys.* **1956**, *24*, 966. Marcus, R. A.; Sutin, N. *Biochim. Biophys. Acta* **1985**, *811*, 265.

(44) Gust, D.; Moore, T. A.; Liddell, P. A.; Nemeth, G. A.; Makings, L. R.; Moore, A. L.; Barrett, D.; Pessiki, P. J.; Bensasson, R. V.; Rougée, M.; Chachaty, C.; De Schryver, F. C.; Van der Auweraer, M.; Holzwarth, A. R.; Connolly, J. S. *J. Am. Chem. Soc.* **1987**, *109*, 846.

by about 0.18 eV but leaves the energies of the lowest lying excited singlet state and the final charge-separated state essentially unchanged. Thus, the thermodynamic driving force for step 8 is increased in **2**. To the extent that charge recombination of $C-P^{\bullet+}-P_F^{\bullet-}$ lies in the inverted region of the Marcus relationship,[43] this step should be slower in **2** than in **1**. Both of these effects should contribute to an enhanced efficiency for step 8. On the other hand, the reduced driving force for steps 5 and 6 in **2**, relative to **1**, results in slower photoinitiated electron transfer (Table II) and consequently a reduced quantum yield of $C-P^{\bullet+}-P_F^{\bullet-}$ relative to that of the corresponding state in **1**.

The long lifetimes found for the $C^{\bullet+}-P-P^{\bullet-}$ states in **1** and **2** are doubtless due to the large spatial separation between the positive and negative charges. The charge recombination reaction could in principle be either a direct process, via step 9 in the schemes, or a two-step process involving a return to intermediate $C-P^{\bullet+}-P^{\bullet-}$ (or $C^{\bullet+}-P^{\bullet-}-P$) states. The spin dynamics of the charge-separated states might also play a role in recombination. The similarity of lifetimes noted for the final states in **1** and **2** suggests that the lifetimes are not being controlled by the energy gap between $C-P^{\bullet+}-P^{\bullet-}$ and $C^{\bullet+}-P-P^{\bullet-}$ or $C^{\bullet+}-P^{\bullet-}-P$ and $C^{\bullet+}-P-P^{\bullet-}$, as these gaps are quite different in the two triads. The simplest explanation is that the charge recombination involves direct electron transfer from the fluorinated porphyrin to the carotenoid, which could be facilitated by the central porphyrin through, for example, superexchange interactions.[45]

The results indicate that, in all of the dyads and triads studied here, the quantum yield of charge separation is being limited substantially by the slow rate of the photodriven electron transfer reactions. This limitation could be overcome either by designing molecules with increased thermodynamic driving force for the reactions in question or by increasing the electron-transfer rate constant by enhancing the degree of electronic coupling between the donor and acceptor. If this can be achieved, then the long lifetimes and relatively high overall quantum yields observed for the triads **1** and **2** suggest that molecules of this type could form the basis of very successful multicomponent photovoltaic molecules.

Experimental Section

Spectroscopic Measurements. The ^1H NMR spectra were obtained at 400 or 500 MHz and refer to ≤1% solutions in chloroform-*d* with tetramethylsilane as an internal reference. The numbering system for identifying the NMR resonances of the porphyrins and carotenoids has been previously reported.[44] The UV–vis spectra were recorded on a Hewlett-Packard 8450A spectrophotometer. Cyclic voltammetric measurements were carried out on a PAR Model 173 potentiostat/galvanostat. All electrochemical measurements were done in 1,2-dichloroethane or dichloromethane at ambient temperatures unless otherwise noted. For transient absorption studies, samples were dissolved in dichloromethane that had been distilled and stored over anhydrous potassium carbonate to remove any HCl, and the resulting solutions were placed in 1 cm × 1 cm × 4 cm cuvettes. The apparatus used for the transient absorption studies features excitation with ca. 15-ns pulses of less than 1 mJ at 590 nm. An adequate signal to noise ratio was achieved by signal averaging (typically for about 500 flashes). The details of the spectrometer have been described elsewhere.[46,47] Quantum yields were determined by a comparative method based on the extinction coefficients of the tetratolylporphyrin triplet state and the carotenoid radical cation as previously described.[48] Fluorescence decay measurements were made on ca. 1×10^{-5} M solutions in dichloromethane with use of the time-correlated single-photon counting method. Two different spectrometers were used. In one, the excitation source was a mode-locked argon ion laser coupled to a synchronously pumped, cavity dumped dye laser operating at 590 nm. Experimental details are provided elsewhere.[49] In the other, the excitation source was a frequency-doubled, mode-locked Nd-YAG laser coupled to a synchronously pumped, cavity dumped dye laser with excitation at 590 nm. Detection was via a microchannel plate photomultiplier (Hamamatsu R2809U-01), and the instrument response time was ca. 35 ps.[50]

The syntheses of **5,15-bis(4-acetamidophenyl)-10,20-bis(4-methylphenyl)porphyrin (8)**,[44] **5,15-bis(4-carbomethoxyphenyl)-10,20-bis(4-methylphenyl)porphyrin (9)**,[51] **13**,[44] **5-(4-acetamidophenyl)-10,15,20-tris(4-methylphenyl)porphyrin (14)**,[44] and **5-(4-aminophenyl)-10,15,20-tris(4-methylphenyl)porphyrin (19)**[52] have been previously reported.

Zinc 5-(4-Acetamidophenyl)-10,15,20-tris(4-methylphenyl)porphyrin (10). To a 50-mL flask were added 7.5 mg (0.011 mmol) of **14** and 10 mL of a 0.04 M solution of $ZnAc_2$ in 80:20 (V/V) dichloromethane/methanol. After it was stirred for 30 min, the solution was chromatographed on a short silica gel column with the same solvent mixture to remove excess $ZnAc_2$ and the solvents were evaporated at reduced pressure. The yield of **10** was 7.4 mg (87%): UV–vis absorption (dichloromethane) λ_{max} (nm) 422, 550, 592; fluorescence emission (λ_{ex} = 550 nm in dichloromethane) λ_{max} (nm) 600, 648.

5-(4-Carbomethoxyphenyl)-10,15,20-tris(pentafluorophenyl)porphyrin (11) was prepared via a modification of the porphyrin synthesis developed by Lindsey and co-workers.[53] In a 2-L round-bottom flask were placed 1.20 g (18 mmol) of pyrrole, 2.65 g (13.5 mmol) of pentafluorobenzaldehyde, and 0.74 g (4.5 mmol) of methyl 4-formylbenzoate together with 1.4 mL of trifluoroacetic acid (TFA) and 1.8 L of chloroform. After the mixture was refluxed for 4.5 h and cooled to room temperature, 4.09 g of 2,3-dichloro-5,6-dicyano-1,4-benzoquinone (DDQ) was added to the mixture and it was stirred overnight. The reaction mixture was neutralized with sodium bicarbonate and extracted with four 100-mL portions of dichloromethane. The organic layer was separated, and the solvent was removed in vacuo. After the solution was filtered through a short silica gel column to remove tars, the porphyrins were separated by chromatography on silica gel with toluene elution. Recrystallization from dichloromethane and methanol gave 61 mg of pure **11** (1.49% yield): ^1H NMR (400 MHz, $CDCl_3$): δ 8.80–8.90 (8 H, m, pyrrole-H), 8.46 (2 H, d, *J* = 8.0 Hz, 5Ar3-H and 5-H), 8.31 (2 H, d, *J* = 8.0 Hz, 5Ar2-H and 6-H), 4.13 (3 H, s, 5Ar-$COOCH_3$), −2.80 (2 H, s, pyrrole-NH); mass spectrum (EI) *m/e* 942 (M^+); UV–vis absorption (dichloromethane) λ_{max} (nm) 414, 510, 540, 586, 640; fluorescence emission (λ_{ex} = 590 nm in dichloromethane) λ_{max} (nm) 643, 713.

Zinc 5,15-Bis(4-acetamidophenyl)-10,20-bis(4-methylphenyl)porphyrin (15) was prepared from 10.3 mg (0.014 mmol) of **8** via the method described for **10**. The yield of **15** was 10.2 mg (93%): UV–vis absorption (dichloromethane) λ_{max} (nm) 422, 550, 592.

Zinc Carotenoporphyrin 16. To a 50-mL flask were added 8.0 mg (0.0067 mmol) of carotenoporphyrin **13** and 10 mL of a 0.04 M solution of $ZnAc_2$ in 80:20 (V/V) dichloromethane/methanol. After it was stirred for 30 min, the solution was chromatographed on a short silica gel column with the same solvent mixture to remove excess $ZnAc_2$ and the solvents were distilled at reduced pressure. The yield of **16** was 96% (8.1 mg): ^1H NMR (400 MHz, $CDCl_3$) δ 8.86–8.98 (8 H, m, pyrrole-H), 8.22 (2 H, d, *J* = 8.4 Hz, 15Ar2-H and 6-H), 8.17 (1 H, s, 15Ar-NH), 8.10 (4 H, d, *J* = 7.8 Hz, 10,20Ar2-H and 6-H), 8.04 (2 H, d, *J* = 8.4 Hz, 15Ar3-H and 5-H), 8.01 (2 H, d, *J* = 8.4 Hz, 2′C-H and 4′C-H), 7.99 (2 H, d, *J* = 8.2 Hz, 5Ar2-H and 6-H), 7.63 (2 H, d, *J* = 8.4 Hz, 1′C-H and 5′C-H), 7.55 (4 H, d, *J* = 7.8 Hz, 10,20Ar3-H and 5-H), 7.06 (2 H, d, *J* = 8.2 Hz, 5Ar3-H and 5-H), 7.06 (1 H, d, *J* = 15.8 Hz, 7′C-H), 6.60–6.70 (4 H, m, 11C-H, 11′C-H, 15C-H, 15′C-H), 6.65 (1 H, d, *J* = 15.8 Hz, 8′C-H), 6.48 (1 H, d, *J* = 15.1 Hz, 12′C-H), 6.44 (1 H, d, *J* = 12.2 Hz, 10′C-H), 6.36 (1 H, d, *J* = 15.0 Hz, 12C-H), 6.33 (1 H, d, *J* = 11.7 Hz, 14′C-H), 6.27 (1 H, d, *J* = 10.0 Hz, 14C-H), 6.19 (1 H, d, *J* = 15.9 Hz, 7C-H), 6.16 (1 H, d, *J* = 7.2 Hz, 10C-H), 6.13 (1 H, d, *J* = 15.9 Hz, 8C-H), 2.71 (6 H, s, 10,20Ar-CH_3), 2.09 (3 H, s, 19′C-CH_3), 2.03 (2 H, m, 4C-CH_2), 2.01 (3 H, s, 20′C-CH_3), 1.99 (3 H, s, 20C-CH_3), 1.98 (3 H, s, 19C-CH_3), 1.72 (3 H, s, 18C-CH_3), 1.60–1.63 (2 H, m, 3C-CH_2), 1.47–1.50 (2 H, m, 2C-CH_2), 1.05 (3 H, s, 16C-CH_3), 1.03 (3 H, s, 17C-CH_3); UV–vis absorption (dichloromethane) λ_{max} (nm) 424, 480, 516, 550, 592; fluorescence emission (λ_{ex} = 530 nm, dichloromethane) λ_{max} (nm) 600, 650.

Triad 2. A 75-mg (0.080 mmol) sample of porphyrin **11** was hydrolyzed to its acid by refluxing in 10 mL of 6 N HCl and 1 mL of trifluoroacetic acid for 4 days, neutralizing to approximately pH 7 with 1% aqueous NaOH, and extracting with chloroform. The chloroform was

---

(45) Sessler, J. L.; Johnson, M. R.; Lin, T.-Y. *Tetrahedron* **1989**, *45*, 4767.

(46) Gust, D.; Moore, T. A.; Makings, L. R.; Liddell, P. A.; Nemeth, G. A.; Moore, A. L. *J. Am. Chem. Soc.* **1986**, *108*, 8028–8031.

(47) Davis, F. S.; Nemeth, G. A.; Anjo, D. M.; Makings, L. R.; Gust, D.; Moore, T. A. *Rev. Sci. Instrum.* **1987**, *58*, 1629.

(48) Moore, T. A.; Gust, D.; Mathis, P.; Mialocq, J. C.; Chachaty, C.; Bensasson, R. V.; Land, E. J.; Doizi, D.; Liddell, P. A.; Nemeth, G. A.; Moore, A. L. *Nature (London)* **1984**, *307*, 630.

(49) Boens, N.; Van den Zegel, M.; De Schryver, F. C. *Chem. Phys. Lett.* **1984**, *111*, 340.

(50) Gust, D.; Moore, T. A.; Luttrull, D. K.; Seely, G. R.; Bittersmann, E.; Bensasson, R. V.; Rougée, M.; Land, E. J.; De Schryver, F. C.; Van der Auweraer, M. *Photochem. Photobiol.* **1990**, *51*, 419.

(51) Anton, J. A.; Loach, P. A. *J. Heterocycl. Chem.* **1975**, *12*, 573.

(52) More, K. M.; Sawant, B. M.; Eaton, G. R.; Eaton, S. S. *Inorg. Chem.* **1981**, *20*, 3354.

(53) Lindsey, J. S.; Hsu, H. C.; Schreiman, I. C. *Tetrahedron Lett.* **1986**, *27*, 4969.

removed by distillation at reduced pressure to yield the pure acid. A total of 71.2 mg of acid **17** was obtained (96% yield).

To a 50-mL flask were added 10 mg (0.011 mmol) of **17**, 10 mL of toluene, 0.50 mL of pyridine, and 0.1 mL (1.37 mmol) of thionyl chloride. The mixture was stirred for 20 min before evaporating the solvent at reduced pressure. A 10-mL portion of toluene was added to the residue, and the solvent was again evaporated under reduced pressure to remove all traces of thionyl chloride. The resulting acid chloride **18** was dissolved in toluene (10 mL), and the solution was added to a solution of 6 mg (0.005 mmol) of **13** dissolved in a mixture of toluene (2 mL) and pyridine (0.5 mL). The reaction mixture was stirred for 13 h under nitrogen before evaporation of the solvent at reduced pressure. The resulting residue was dissolved in a mixture of water and dichloromethane and extracted with dichloromethane. The organic layer was evaporated to dryness and dissolved in toluene, and the toluene was distilled in order to remove any residual water and pyridine. The residue was chromatographed on silica gel (2% acetone in dichloromethane) to yield 6.5 mg of pure triad **2** (62% yield): ^{1}H NMR (400 MHz, $CDCl_3$) δ 8.89–9.01 (16 H, m, pyrrole-H), 8.51 (1 H, s, 5Ar-NH), 8.47 (2 H, AB, J = 9.0 Hz, 15Ar2-H and 6-H), 8.46 (2 H, AB, J = 9.0 Hz, 15Ar3-H and 5-H), 8.34 (2 H, d, J = 8.4 Hz, 5′Ar3-H and 5-H), 8.25 (2 H, d, J = 8.4 Hz, 5Ar2-H and 6-H), 8.23 (2 H, d, J = 8.4 Hz, 5′Ar2-H and 6-H), 8.16 (1 H, s, 15Ar-NH), 8.13 (4 H, d, J = 8.4 Hz, 10,20Ar2-H and 6-H), 8.07 (2 H, d, J = 8.4 Hz, 5Ar3-H and 5-H), 8.01 (2 H, d, J = 8.4 Hz, 2′C-H and 4′C-H), 7.63 (2 H, d, J = 8.4 Hz, 1′C-H and 5′C-H), 7.59 (4 H, d, J = 8.4 Hz, 10,20Ar3-H and 5-H), 7.06 (1 H, d, J = 15.8 Hz, 7′C-H), 6.60–6.70 (4 H, m, 11C-H, 11′C-H, 15C-H, 15′C-H), 6.65 (1 H, d, J = 15.8 Hz, 8′C-H), 6.48 (1 H, d, J = 15.1 Hz, 12′C-H), 6.44 (1 H, d, J = 12.2 Hz, 10′C-H), 6.36 (1 H, d, J = 15.0 Hz, 12C-H), 6.33 (1 H, d, J = 11.7 Hz, 14′C-H), 6.27 (1 H, d, J = 10.0 Hz, 14C-H), 6.19 (1 H, d, J = 15.9 Hz, 7C-H), 6.16 (1 H, d, J = 7.2 Hz, 10C-H), 6.13 (1 H, d, J = 15.9 Hz, 8C-H), 2.71 (6 H, s, 10,20Ar-CH_3), 2.09 (3 H, s, 19′C-CH_3), 2.03 (2 H, m, 4C-CH_2), 2.01 (3 H, s, 20′C-CH_3), 1.99 (3 H, s, 20C-CH_3), 1.98 (3 H, s, 19C-CH_3), 1.72 (3 H, s, 18C-CH_3), 1.60–1.63 (2 H, m, 3C-CH_2), 1.47–1.50 (2 H, m, 2C-CH_2), 1.05 (3 H, s, 16C-CH_3), 1.03 (3 H, s, 17C-CH_3), −2.78 (2 H, s, pyrrole-NH), −2.87 (2 H, s, pyrrole-NH); UV–vis absorption (dichloromethane) λ_{max} (nm) 422, 482, 512, 588, 650; fluorescence emission (λ_{ex} = 590 nm, dichloromethane) λ_{max} (nm) 656, 718.

Triad 1 was prepared with use of a procedure identical with that described above for **2**, with 10.0 mg (0.0080 mmol) of **16**. A total of 12.1 mg of **1** was obtained (71% yield): ^{1}H NMR (400 MHz, $CDCl_3$) δ 8.89–9.05 (16 H, m, pyrrole-H), 8.51 (1 H, s, 5Ar-NH), 8.46 (4 H, s, 15Ar2-H, 3-H, 5-H and 6-H), 8.34 (2 H, d, J = 8.4 Hz, 5′Ar3-H and 5-H), 8.25 (2 H, d, J = 8.4 Hz, 5Ar2-H and 6-H), 8.23 (2 H, d, J = 8.4 Hz, 5′Ar2-H and 6-H), 8.16 (1 H, s, 15Ar-NH), 8.13 (4 H, d, J = 8.4 Hz, 10,20Ar2-H and 6-H), 8.07 (2 H, d, J = 8.4 Hz, 5Ar3-H and 5-H), 8.01 (2 H, d, J = 8.4 Hz, 2′C-H and 4′C-H), 7.63 (2 H, d, J = 8.4 Hz, 1′C-H and 5′C-H), 7.59 (4 H, d, J = 8.4 Hz, 10,20Ar3-H and 5-H), 7.06 (1 H, d, J = 15.8 Hz, 7′C-H), 6.60–6.70 (4 H, m, 11C-H, 11′C-H, 15C-H, 15′C-H), 6.65 (1 H, d, J = 15.8 Hz, 8′C-H), 6.48 (1 H, d, J = 15.1 Hz, 12′C-H), 6.44 (1 H, d, J = 12.2 Hz, 10′C-H), 6.36 (1 H, d, J = 15.0 Hz, 12C-H), 6.33 (1 H, d, J = 11.7 Hz, 14′C-H), 6.27 (1 H, d, J = 10.0 Hz, 14C-H), 6.19 (1 H, d, J = 15.9 Hz, 7C-H), 6.16 (1 H, d, J = 7.2 Hz, 10C-H), 6.13 (1 H, d, J = 15.9 Hz, 8C-H), 2.71 (6 H, s, 10,20Ar-CH_3), 2.09 (3 H, s, 19′C-CH_3), 2.03 (2 H, m, 4C-CH_2), 2.01 (3 H, s, 20′C-CH_3), 1.99 (3 H, s, 20C-CH_3), 1.98 (3 H, s, 19C-CH_3), 1.72 (3 H, s, 18C-CH_3), 1.60–1.63 (2 H, m, 3C-CH_2), 1.47–1.50 (2 H, m, 2C-CH_2), 1.05 (3 H, s, 16C-CH_3), 1.03 (3 H, s, 17C-CH_3), −2.78 (2 H, s, pyrrole-NH); UV–vis absorption (dichloromethane) λ_{max} (nm) 422, 482, 508, 588, 640; fluorescence emission (λ_{ex} = 425 nm, dichloromethane) λ_{max} (nm) 641, 709.

Carotenoporphyrin 12. Carotenoporphyrin **16** (~3 mg, 0.002 mmol) was dissolved in 2 mL of dry pyridine, and a few drops of acetic anhydride were added. After just a few minutes, TLC of the sample on silica gel with 5% ethyl acetate in toluene indicated the quantitative formation of a product more polar than the starting material. The mixture was diluted with chloroform and extracted one time with a saturated solution of sodium bicarbonate and two times with water. Flash column chromatography on silica gel with 1–2% methanol in chloroform afforded pure **12** in essentially quantitative yield: ^{1}H NMR (400 MHz, $CDCl_3$) δ 8.91–8.97 (8 H, m, pyrrole-H), 8.21 (2 H, d, J = 8.4 Hz, 15Ar2-H and 6-H), 8.14 (2 H, d, J = 8.2 Hz, 5Ar2-H and 6-H), 8.10 (4 H, d, J = 7.9 Hz, 10,20Ar2-H and 6-H), 7.97 (2 H, d, J = 8.4 Hz, 15Ar3-H and 5-H), 7.91 (2 H, d, J = 8.5 Hz, 2′C-H and 4′C-H), 7.76 (2 H, d, J = 8.2 Hz, 5Ar3-H and 5-H), 7.60 (2 H, d, J = 8.5 Hz, 1′C-H and 5′C-H), 7.55 (4 H, d, J = 7.9 Hz, 10,20Ar3-H and 5-H), 7.05 (1 H, d, J = 16.3 Hz, 7′C-H), 6.65–6.72 (4 H, m, 11C-H, 11′C-H, 15C-H, 15′C-H), 6.64 (1 H, d, J = 16.3 Hz, 8′C-H), 6.47 (1 H, d, J = 15.7 Hz, 12′C-H), 6.44 (1 H, d, J = 12.0 Hz, 10′C-H), 6.36 (1 H, d, J = 14.8 Hz, 12C-H), 6.33 (1 H, d, J = 9.4 Hz, 14′C-H), 6.28 (1 H, d, J = 10.4 Hz, 14C-H), 6.19 (1 H, d, J = 17.2 Hz, 7C-H), 6.16 (1 H, d, J = 7.3 Hz, 10C-H), 6.13 (1 H, d, J = 17.2 Hz, 8C-H), 5.11 (1 H, s, 15Ar-NH), 2.72 (6 H, s, 10,20Ar-CH_3), 2.22 (3 H, s, $COCH_3$), 2.09 (3 H, s, 19′C-CH_3), 2.02 (2 H, m, 4C-CH_2), 2.00 (3 H, s, 20′C-CH_3), 1.99 (3 H, s, 20C-CH_3), 1.98 (3 H, s, 19C-CH_3), 1.72 (3 H, s, 18C-CH_3), 1.61–1.63 (2 H, m, 3C-CH_2), 1.45–1.48 (2 H, m, 2C-CH_2), 1.05 (3 H, s, 16C-CH_3), 1.03 (3 H, s, 17C-CH_3); UV–vis absorption (dichloromethane) λ_{max} (nm) 422, 482, 508, 588; fluorescence emission (λ_{ex} = 590 nm in dichloromethane) λ_{max} (nm) 600, 648.

Diporphyrin 3. A 78-mg portion (0.103 mmol) of the diester **9** was stirred with 3 mL of concentrated aqueous HCl at 90 °C for 4 h. The mixture was neutralized with a saturated solution of sodium bicarbonate and filtered to separate the solid porphyrins from the aqueous solution. Flash chromatography of the porphyrin mixture on silica gel (0.5% methanol in chloroform) yielded 22.4 mg of the desired 5-(4-carboxyphenyl)-15-(4-carbomethoxyphenyl)-10,20-bis(4-methylphenyl)porphyrin (29%). The acid chloride was obtained by treating 10.5 mg (0.014 mmol) of this porphyrin dissolved in 3 mL of dry toluene and 0.5 mL of dry pyridine with an excess of thionyl chloride. The mixture was stirred for 15 min under nitrogen, and the solvents and excess thionyl chloride were then removed at reduced pressure. The acid chloride was redissolved in 3 mL of toluene and 0.5 mL of pyridine and mixed with 7.6 mg (0.011 mmol) of 5-(4-aminophenyl)-15-(4-acetamidophenyl)-10,20-bis(4-methylphenyl)porphyrin, which was obtained by partial hydrolysis (acid-catalyzed) of **8** followed by column chromatography on silica gel with 1% methanol in chloroform. The mixture was stirred overnight under nitrogen. TLC of a sample of the reaction mixture indicated the quantitative formation of the desired diporphyrin, which was less polar than either of the starting materials. The reaction mixture was diluted with chloroform and extracted two times with a saturated solution of sodium bicarbonate and once with water. The solvent was evaporated under reduced pressure and the residue chromatographed on silica gel (flash column with 0.5% methanol in chloroform) to yield 14.3 mg (93%) of pure **3**: ^{1}H NMR (400 MHz, $CDCl_3$) δ 8.79–8.96 (16 H, m, pyrrole-H), 8.48 (1 H, s, 5Ar-NH), 8.45 (2 H, d, J = 7.8 Hz, 15′Ar2-H and 6-H), 8.31 (2 H, d, J = 7.8 Hz, 15′Ar3-H and 5-H), 8.43 (4 H, br s, 5Ar2-H, 3-H, 5-H and 6-H), 8.31 (2 H, d, J = 8.0 Hz, 5′Ar2-H and 6-H), 8.20 (2 H, d, J = 8.0 Hz, 5′Ar3-H and 5-H), 8.17 (2 H, d, J = 7.9 Hz, 15Ar2-H and 6-H), 7.89 (2 H, d, J = 7.9 Hz, 15Ar3-H and 5-H), 8.12 (8 H, d, J = 7.9 Hz, 10,20,10′,20′Ar2-H and 6-H), 7.58 (8 H, d, J = 7.9 Hz, 10,20,10′,20′Ar3-H and 5-H), 7.46 (1 H, s, 15Ar-NH), 4.12 (3 H, s, OCH_3), 2.72 (12 H, s, Ar-CH_3), 2.36 (3 H, s, $COCH_3$); UV–vis absorption (dichloromethane) λ_{max} (nm) 422, 518, 554, 594, 650; fluorescence emission (λ_{ex} = 420 nm in dichloromethane) λ_{max} (nm) 655, 720.

Diporphyrin 4. The acid chloride was prepared as described in the preparation of **3** starting with 10.6 mg (0.014 mmol) of the monoacid–porphyrin obtained by partial hydrolysis (acid-catalyzed) of the diester **9**. The acid chloride was dissolved in 3 mL of dry toluene and 1 mL of dry pyridine. The zinc derivative of 5-(4-aminophenyl)-15-(4-acetamidophenyl)-10,20-bis(4-methylphenyl)porphyrin (5.6 mg (0.007 mmol)) was dissolved in 1 mL each of toluene and pyridine and added at once to the stirred solution of the acid chloride. The entire operation was done under argon. The reaction appeared essentially complete after a few minutes. Thin-layer chromatographic analysis showed that the desired dyad had an R_f of 0.5 on a silica gel plate with 5% methanol in chloroform. A nonpolar porphyrin-like material was also visible on the TLC (R_f ca. 0.9) but disappeared after 12 h. The final purification was accomplished by flash chromatography on silica gel with chloroform as the solvent, and 6.8 mg of pure **4** (63% yield) was isolated: ^{1}H NMR (400 MHz, $CDCl_3$) δ 8.79–9.06 (16 H, m, pyrrole-H), 8.51 (1 H, s, 5Ar-NH), 8.45 (2 H, d, J = 7.8 Hz, 15′Ar2-H and 6-H), 8.33 (2 H, d, J = 7.8 Hz, 15′Ar3-H and 5-H), 8.45 (4 H, m, 5Ar2-H, 3-H, 5-H and 6-H), 8.32 (2 H, d, J = 8.3 Hz, 5′Ar2-H and 6-H), 8.21 (2 H, d, J = 8.3 Hz, 5′Ar3-H and 5-H), 8.19 (2 H, d, J = 8.3 Hz, 15Ar2-H and 6-H), 7.90 (2 H, d, J = 8.3 Hz, 15Ar3-H and 5-H), 8.12 (8 H, d, J = 7.9 Hz, 10,20,10′,20′Ar2-H and 6-H), 7.58 (8 H, d, J = 7.9 Hz, 10,20,10′,20′Ar3-H and 5-H), 7.49 (1 H, s, 15Ar-NH), 4.12 (3 H, s, OCH_3), 2.73 (12 H, s, Ar-CH_3), 2.36 (3 H, s, $COCH_3$), −2.74 (2 H, s, NH′); UV–vis absorption (dichloromethane) λ_{max} (nm) 422, 512, 552, 590, 650; fluorescence emission (λ_{ex} = 550 nm in dichloromethane) λ_{max} (nm) 655, 720.

Diporphyrin 5. The acid chloride of **17** was prepared as described for the synthesis of **2** starting with 25 mg of the acid (0.027 mmol). An excess of 5,15-bis(4-aminophenyl)-10,20-bis(4-methylphenyl)porphyrin[44] (29.4 mg, 0.044 mmol), dissolved in 2 mL of toluene and 0.5 mL of pyridine, was rapidly added to the acid chloride. The reaction was instantaneous. After dilution with chloroform and extraction with sodium bicarbonate solution and water, column chromatography on silica gel with 0.5% acetone in dichloromethane afforded 13.7 mg (32%) of the desired dyad. The free amino group of the dyad was acetylated to yield **5** by simply dissolving the aminodyad in 2 mL of acetic anhydride and five drops of pyridine. The mixture was allowed to stand for 1 h. Following dilution with chloroform, extraction with a saturated solution of sodium bicarbonate, two extractions with water, and evaporation of the solvents at reduced pressure, the residue was purified by column chromatography on silica gel with chloroform to yield quantitatively diporphyrin **5**: ^{1}H NMR (400 MHz, $CDCl_3$) δ 8.85–9.01 (16 H, m, pyrrole-H), 8.49 (1 H, s, 5Ar-NH), 8.45 (4 H, AB, $J = 8.2$ Hz, 5Ar2-H, 3-H, 5-H and 6-H), 8.33 (2 H, d, $J = 8.4$ Hz, 5′Ar2-H and 6-H), 8.20 (2 H, d, $J = 8.4$ Hz, 5′Ar3-H and 5-H), 8.17 (2 H, d, $J = 8.2$ Hz, 15Ar2-H and 6-H), 7.88 (2 H, d, $J = 8.2$ Hz, 15Ar3-H and 5-H), 8.11 (4 H, d, $J = 7.9$ Hz, 10, 20Ar2-H and 6-H), 7.57 (4 H, d, $J = 7.9$ Hz, 10,20Ar3-H and 5-H), 7.46 (1 H, s, 15Ar-NH), 2.72 (6 H, s, Ar-CH_3), 2.35 (3 H, s, $COCH_3$), –2.72 (2 H, s, NH′), –2.81 (2 H, s, NH); UV–vis absorption (dichloromethane) λ_{max} (nm) 420, 512, 554, 590, 650; fluorescence emission (λ_{ex} = 590 nm in dichloromethane) λ_{max} (nm) 655, 718.

Diporphyrin 6. Freshly prepared acid chloride **18** (from 30 mg (0.032 mmol) of the acid) was dissolved in 10 mL of toluene, and the resulting solution was added to 8.0 mg (0.012 mmol) of **19** dissolved in a mixture of toluene (2 mL) and pyridine (0.5 mL). The mixture was stirred for 5 h, and the solvent was then distilled at reduced pressure. The residue was dissolved in water and dichloromethane and extracted with dichloromethane. The organic layer was evaporated to dryness, the residue dissolved in toluene, and the resulting solution distilled to remove any residual water and pyridine. The residue was purified by chromatography on silica gel (dichloromethane) and recrystallization from dichloromethane and methanol to give 18 mg of compound **6** (95% yield): ^{1}H NMR (400 MHz, $CDCl_3$) δ 8.88–9.01 (16 H, m, pyrrole-H), 8.50 (1 H, s, 5Ar-NH), 8.46 (2 H, AB, $J = 9.0$ Hz, 5Ar3-H, and 5-H), 8.47 (2 H, AB $J = 9.0$ Hz, 5Ar2-H and 6-H), 8.34 (2 H, d, $J = 8.4$ Hz, 5′Ar3-H and 5-H), 8.22 (2 H, d, $J = 8.4$ Hz, 5′Ar2-H and 6-H), 8.13 (4 H, d, $J = 7.6$ Hz, 10,20Ar2-H and 6-H), 8.11 (2 H, d, $J = 7.0$ Hz, 15Ar2-H and 6-H), 7.58 (4 H, d, $J = 7.6$ Hz, 10,20Ar3-H and 5-H), 7.56 (2 H, d, $J = 7.0$ Hz, 15Ar3-H and 5-H), 2.72 (6 H, s, 10,20Ar-CH_3), 2.71 (3 H, s, 10,15,20Ar-CH_3), –2.87 (2 H, s, pyrrole-NH), –2.78 (2 H, s, PF15 pyrrole-NH); UV–vis absorption (dichloromethane) λ_{max} (nm), 420, 514, 552, 590, 648; fluorescence emission (λ_{ex} = 590 nm, dichloromethane) λ_{max} (nm), 652, 718.

Zinc 5-(4-Aminophenyl)-10,15,20-tris(4-methylphenyl)porphyrin (20) was prepared from 15 mg (0.022 mmol) of **19** via the method described for **10**. The yield was 14 mg (86%): UV–vis absorption (dichloromethane) λ_{max} (nm) 422, 550, 590; fluorescence emission (λ_{ex} = 550 nm in dichloromethane) λ_{max} (nm) 603, 649.

Diporphyrin 7. Freshly prepared acid chloride **18** (from 20 mg (0.022 mmol) of the acid) was dissolved in 10 mL of toluene, and the resulting solution was added to 7.4 mg (0.010 mmol) of **20** dissolved in a mixture of toluene (2 mL) and pyridine (2 mL). The mixture was stirred for 14 h, and the solvents were then evaporated at reduced pressure. The residue was dissolved in dichloromethane and extracted with water. The organic layer was evaporated to dryness, the residue dissolved in toluene, and the resulting solution distilled to remove any residual water and pyridine. The residue was purified by chromatography on silica gel (dichloromethane) and recrystallization from dichloromethane and methanol to give 9.0 mg of **7** (54% yield): ^{1}H NMR (400 MHz, $CDCl_3$) δ 8.95–9.02 (16 H, m, pyrrole-H), 8.50 (1 H, s, 5Ar-NH), 8.46 (2 H, AB, $J = 9.0$ Hz, 5Ar3-H, and 5-H), 8.47 (2 H, AB, $J = 9.0$ Hz, 5Ar2-H and 6-H), 8.34 (2 H, d, $J = 8.4$ Hz, 5′Ar3-H and 5-H), 8.22 (2 H, d, $J = 8.4$ Hz, 5′Ar2-H and 6-H), 8.13 (4 H, d, $J = 7.6$ Hz, 10,20Ar2-H and 6-H), 8.11 (2 H, d, $J = 7.0$ Hz, 15Ar2-H and 6-H), 7.58 (4 H, d, $J = 7.6$ Hz, 10,20Ar3-H and 5-H), 7.56 (2 H, d, $J = 7.0$ Hz, 15Ar3-H and 5-H), 2.72 (6 H, s, 10,20Ar-CH_3), 2.71 (3 H, s, 15Ar-CH_3), –2.78 (2 H, s, PF15 pyrrole-NH); UV–vis absorption (dichloromethane) λ_{max} (nm), 422, 510, 550, 588, 640; fluorescence emission (λ_{ex} = 550 nm, dichloromethane) λ_{max} (nm), 600, 643, 710.

Acknowledgment. This research was supported by the National Science Foundation (Grant CHE-8903216) and the Department of Energy University Research Instrumentation Program (Grant DE-FG05-87ER75361). This is publication 64 from the Arizona State University Center for the Study of Early Events in Photosynthesis. The Center is funded by U. S. Department of Energy Grant DE-FG02-88ER13969 as part of the U. S. Department of Agriculture-Department of Energy-National Science Foundation Plant Science Center Program.

Tetramethylene Dications $(CH_2)_4^{2+}$: Are the Norbornadiene Dication, the Pagodane Dication, and Related Systems Aromatic?[‖]

Rainer Herges,[*,†] Paul von Ragué Schleyer,[†] Michael Schindler,[‡] and Wolf-Dieter Fessner[§]

Contribution from the Institut für Organische Chemie der Friedrich-Alexander, Universität Erlangen-Nürnberg, 8520 Erlangen, West Germany, Bayer AG, Zentrale Forschung und Entwicklung, 5090 Leverkusen, West Germany, and Institut für Organische Chemie und Biochemie der Universität Freiburg, Freiburg, West Germany. *Received January 3, 1990*

Abstract: The $(CH_2)_4^{2+}$ potential energy hypersurface has been investigated by semiempirical and ab initio calculations. The global minimum is an acyclic structure of C_i symmetry. Harmonic vibrational analysis of the rectangular cyclobutane dication (D_{2h}), which serves as a model for "σ-aromatic" pagodane and norbornadiene dications, indicates three imaginary frequencies. Nonetheless, strong evidence that the pagodane dication has a nonclassical, "aromatic" structure of D_{2h} symmetry is presented. A rapid equilibrium of two classical C_{2v} structures and a diradical D_{2h} species, in which both are consistent with the experimental NMR spectroscopic data, can be excluded on the basis of our theoretical investigations. The norbornadiene dication is also predicted to be stabilized by aromaticity, whereas structures with larger distances between the two formal ethylene radical cations are predicted to exhibit increasing diradicaloid character.

Treated at –80 °C with SbF_5/SO_2ClF, [1.1.1.1]pagodane (**1**) is oxidized to give a dication persistent for several hours at room temperature.[1] This behavior is remarkable since no stabilizing aromatic or heteroatomic substituents are present. ^{13}C and ^{1}H NMR spectra indicate the preservation of the original D_{2h} symmetry at least on the observational time scale. Quenching **1** with methanol yields the decacyclic derivative **2**. The remarkable stability of the dication implies an extraordinary electronic

---

[‖] Dedicated to H. Prinzbach on the occasion of his 60th birthday.

[†] Universität Erlangen-Nürnberg.

[‡] Bayer AG.

[§] Universität Freiburg.

(1) (a) Prakash, G. K. S.; Krishnamurthy, V. V.; Herges, R.; Bau, R.; Yuan, H.; Olah, G. A.; Fessner, W.-D.; Prinzbach, H. *J. Am. Chem. Soc.* **1986**, *108*, 836. (b) For review on organic dications, see: Lammertsma, K.; Schleyer, P. v. R.; Schwarz, H. *Angew. Chem., Int. Ed. Engl.* **1989**, *10*, 1321.